Role of the transcriptional regulator SP140 in resistance to bacterial infections via repression of type I interferons

Daisy X. Ji[1*], Kristen C. Witt[1*], Dmitri I. Kotov[1,2], Shally R. Margolis[1], Alexander Louie[1], Victoria Chevée[1], Katherine J. Chen[1,2], Harmandeep S. Dhaliwal[3], Angus Y. Lee[3], Dario S. Zamboni[4], Igor Kramnik[5], Daniel A. Portnoy[1,6,7], K. Heran Darwin[8], Russell E. Vance[1,2,3**]

[1] Division of Immunology and Pathogenesis, Department of Molecular and Cell Biology, University of California, Berkeley, CA 94720 USA

[2] Howard Hughes Medical Institute, University of California, Berkeley, CA 94720 USA

[3] Cancer Research Laboratory, University of California, Berkeley, CA 94720 USA

[4] Department of Cell Biology, Ribeirão Preto Medical School, University of São Paulo, Ribeirão Preto, São Paulo, Brazil.

[5] The National Emerging Infectious Diseases Laboratory, Department of Medicine (Pulmonary Center), and Department of Microbiology, Boston University School of Medicine, Boston, MA, USA.

[6] Division of Biochemistry, Biophysics and Structural Biology, Department of Molecular and Cell Biology, University of California, Berkeley, CA 94720 USA

[7] Department of Plant and Microbial Biology, University of California, Berkeley, CA 94720 USA

[8] Department of Microbiology, New York University Grossman School of Medicine, New York, NY, USA

* These authors contributed equally to this work.

** e-mail: rvance@berkeley.edu

Impact Statement: Repression of type I interferons by SP140 is essential for resistance to *Legionella pneumophila*, and *Mycobacterium tuberculosis*.

Abstract

Type I interferons (IFNs) are essential for anti-viral immunity, but often impair protective immune responses during bacterial infections. An important question is how type I IFNs are strongly induced during viral infections, and yet are appropriately restrained during bacterial infections. The *Super susceptibility to tuberculosis 1* (*Sst1*) locus in mice confers resistance to diverse bacterial infections. Here we provide evidence that *Sp140* is a gene encoded within the *Sst1* locus that represses type I IFN transcription during bacterial infections. We generated *Sp140*$^{-/-}$ mice and find they are susceptible to infection by *Legionella pneumophila* and *Mycobacterium tuberculosis*. Susceptibility of *Sp140*$^{-/-}$ mice to bacterial infection was rescued by crosses to mice lacking the type I IFN receptor (*Ifnar*$^{-/-}$). Our results implicate *Sp140* as an important repressor of type I IFNs that is essential for resistance to bacterial infections.

42 **Introduction**

43 Type I interferons (IFNs) comprise a group of cytokines, including interferon-β and multiple
44 interferon-α isoforms, that are essential for immune defense against most viruses (Stetson and
45 Medzhitov, 2006). Type I IFNs signal through a cell surface receptor, the interferon alpha and
46 beta receptor (IFNAR), to induce an 'anti-viral state' that is characterized by the transcriptional
47 induction of hundreds of interferon stimulated genes (ISGs) (Schneider et al., 2014). Many ISGs
48 encode proteins with direct anti-viral activities. Type I IFNs also promote anti-viral responses by
49 cytotoxic T cells and Natural Killer cells. Accordingly, *Ifnar*$^{-/-}$ mice are highly susceptible to
50 most viral infections.

51 Many ISGs are also induced by IFN-γ (also called type II IFN). However, type I and type
52 II IFNs appear to be specialized for the control of different classes of pathogens (Crisler and
53 Lenz, 2018). Whereas type I IFNs are predominantly anti-viral, the ISGs induced by IFN-γ
54 appears to be especially important for the control of diverse intracellular pathogens, including
55 bacteria and parasites. In contrast, type I IFNs play complex roles during bacterial infections
56 (Boxx and Cheng, 2016; Donovan et al., 2017; McNab et al., 2015; Moreira-Teixeira et al.,
57 2018). Some ISGs induced by type I IFN, most notably certain guanylate binding proteins
58 (GBPs), have anti-bacterial activities (Pilla-Moffett et al., 2016). At the same time, several
59 proteins induced by type I IFNs, including interleukin-10 (IL-10) and IL-1 receptor antagonist
60 (IL-1RA), impair anti-bacterial immunity (Boxx and Cheng, 2016; Ji et al., 2019; Mayer-Barber
61 et al., 2014). As a result, the net effect of type I IFN is often to increase susceptibility to bacterial
62 infections. For example, *Ifnar*$^{-/-}$ mice exhibit enhanced resistance to *Listeria monocytogenes*
63 (Auerbuch et al., 2004; Carrero et al., 2004; O'Connell et al., 2004) and *Mycobacterium*
64 *tuberculosis* (Donovan et al., 2017; Dorhoi et al., 2014; Ji et al., 2019; Mayer-Barber et al., 2014;
65 Moreira-Teixeira et al., 2018). Multiple mechanisms appear to explain resistance of *Ifnar*$^{-/-}$ mice
66 to *L. monocytogenes*, including a negative effect of type I IFNs on protective IFN-γ signaling
67 (Rayamajhi et al., 2010). Likewise, diverse mechanisms underlie the negative effects of type I
68 IFNs during *M. tuberculosis* infection, including alterations of eicosanoid production (Mayer-
69 Barber et al., 2014) and the induction of IL-1Ra (Ji et al., 2019), both of which impair protective
70 IL-1 responses.

71 As an experimental model for dissecting the mechanisms by which inappropriate type I
72 IFN responses are restrained during bacterial infections, we have compared mice harboring
73 different haplotypes of the *Super susceptibility to tuberculosis 1* (*Sst1*) locus (Pan et al., 2005;
74 Pichugin et al., 2009). The *Sst1* locus encompasses about 10M base pairs of mouse chromosome
75 1, a region that contains approximately 50 genes. Mice harboring the susceptible (S) haplotype of
76 *Sst1*, derived from the C3H/HeBFeJ mouse strain, succumb relatively rapidly to *M. tuberculosis*

77 infection as compared to isogenic mice harboring the resistant (R) *Sst1* haplotype (derived from
78 C57BL/6 mice). Likewise, *Sst1*^{S} mice also exhibit enhanced susceptibility to *Listeria*
79 *monocytogenes* (Boyartchuk et al., 2004; Pan et al., 2005) and *Chlamydia pneumoniae* (He et al.,
80 2013). The susceptibility of *Sst1*^{S} mice to *M. tuberculosis* was reversed by crossing to *Ifnar*$^{-/-}$
81 mice (He et al., 2013; Ji et al., 2019), thereby demonstrating the causative role of type I IFNs in
82 driving the susceptibility phenotype. Although multiple type I IFN-induced genes are likely
83 responsible for the detrimental effects of type I IFNs during bacterial infections, heterozygous
84 deficiency of a single type I IFN-induced gene, *Il1rn* (encoding IL-1 receptor antagonist), was
85 sufficient to almost entirely reverse the susceptibility of *Sst1*^{S} mice to *M. tuberculosis* (Ji et al.,
86 2019).

87 The *Sst1*^{R} haplotype is dominant over the *Sst1*^{S} haplotype, suggesting that *Sst1*^{R} likely
88 encodes a protective factor that is absent from *Sst1*^{S} mice (Pan et al., 2005; Pichugin et al., 2009).
89 By comparing gene expression in *Sst1*^{R} versus *Sst1*^{S} mice, *Sp110* (also known as *Ipr1*) was
90 discovered as an *Sst1*-encoded gene that is transcribed selectively in *Sst1*^{R} mice (Pan et al.,
91 2005). Transgenic expression of *Sp110* in *Sst1*^{S} mice partially restored resistance to *M.*
92 *tuberculosis* and *L. monocytogenes* (Pan et al., 2005). However, the causative role of *Sp110* in
93 conferring resistance to bacterial infections was not confirmed by the generation of *Sp110*-
94 deficient B6 mice. Null mutations of human *SP110* are associated with VODI (hepatic veno-
95 occlusive disease with immunodeficiency syndrome, OMIM 235550), but not mycobacterial
96 diseases (Roscioli et al., 2006). Some studies have found polymorphisms in *SP110* to be
97 associated with susceptibility to TB, though not consistently so across different ethnic groups
98 (Chang et al., 2018; Fox et al., 2014; Lei et al., 2012; Png et al., 2012; Thye et al., 2006; Tosh et
99 al., 2006; Zhang et al., 2017).

100 In humans and mice, SP110 is a part of the Speckled Protein (SP) family of nuclear
101 proteins, consisting of SP100, SP110 and SP140 (and SP140L in humans only) (Perniola and
102 Musco, 2014). The SP family members also exhibit a high degree of similarity to AIRE, a
103 transcriptional regulator that promotes tolerance to self-antigens by inducing their expression in
104 thymic epithelial cells (Anderson and Su, 2016; Perniola and Musco, 2014). All members of the
105 SP-AIRE family in both mice and humans have an N-terminal SP100 domain that appears to
106 function as a homotypic protein-protein interaction domain (Fraschilla and Jeffrey, 2020; Huoh
107 *et al*, 2020). The SP100 domain is closely related to the Caspase Activation and Recruitment
108 Domain (CARD), though SP family members are not believed to activate caspases. SP-AIRE
109 proteins also contain a DNA-binding SAND domain (Bottomley et al., 2001). Certain SP
110 isoforms, including all human full-length SP family members and mouse SP140, also include a
111 plant homeobox domain (PHD) and a bromodomain (BRD) (Perniola and Musco, 2014). The

genes encoding SP family proteins are linked in a small cluster in both mouse and human genomes and are inducible by IFN-γ in a variety of cell lines. The mouse *Sp100/110/140* gene cluster is adjacent to a highly repetitive 'homogenously staining region' (HSR) of chromosome 1 that remains poorly assembled in the most recent genome assembly due to the presence of as many as 40 near-identical repeats of *Sp110*-like sequences (Pan et al., 2005; Weichenhan et al., 2001). Most of these repeated *Sp110*-like sequences in the HSR appear to be either incomplete copies of *Sp110* or pseudogenes that are not believed to be translated, but their presence has nevertheless complicated genetic targeting and analysis of the SP gene family.

With the advent of CRISPR–Cas9-based methods (Wang et al., 2013), we were able to generate *Sp110*$^{-/-}$ mice on the B6 background. Surprisingly, we found that *Sp110*$^{-/-}$ mice do not phenocopy the susceptibility of *Sst1*^{S} mice to *M. tuberculosis* infection *in vivo*. Upon analysis of additional candidate genes in the *Sst1* locus, we found that B6.*Sst1*^{S} mice also lack expression of *Sp140*. To test whether loss of *Sp140* might account for the susceptibility of *Sst1*^{S} mice to bacterial infections, we generated *Sp140*$^{-/-}$ mice. We found these mice are as susceptible as B6.*Sst1*^{S} mice to the intracellular bacterial pathogens *M. tuberculosis* and *Legionella pneumophila*. Similar to B6.*Sst1*^{S} mice, *Sp140*$^{-/-}$ mice exhibit an exacerbated type I IFN response after bacterial infection, and the susceptibility of *Sp140*$^{-/-}$ mice is rescued by crosses to *Ifnar*$^{-/-}$ mice. Our results suggest that loss of *Sp140* explains the susceptibility to bacterial infections associated with the *Sst1*^{S} haplotype. These data further suggest that SP140 is a novel negative regulator of type I IFN responses that is essential for protection against intracellular bacterial infections.

Results

Sp110*$^{-/-}$ mice are not susceptible to *M. tuberculosis. Loss of *Sp110* expression was proposed to account for the susceptibility of mice carrying the *Sst1*^{S} haplotype to bacterial infections (Pan et al., 2005). We first confirmed that bone marrow-derived macrophages (BMMs) from B6.*Sst1*^{S} mice lack expression of *Sp110* protein (Figure 1A). To determine whether loss of *Sp110* confers susceptibility to bacterial infections, we used CRISPR–Cas9 to target exon 3 of *Sp110* to generate *Sp110*$^{-/-}$ mice on the C57BL/6 (B6) background (Figure 1– figure supplement 1). We generated three independent *Sp110*$^{-/-}$ lines, denoted as lines 61, 65 and 71 (Figure 1A, Figure 1– figure supplement 1). All three lines lacked expression of *Sp110*, as verified using three different antibodies (Figure 1A). *Sp110*$^{-/-}$ mice are viable and are born at normal Mendelian ratios and litter sizes. When aerosol infected with a low-dose of *M. tuberculosis*, *Sp110*$^{-/-}$ mice did not phenocopy the susceptibility observed in B6.*Sst1*^{S} mice (Figure 1B-D). At day 25 post-infection,

146 *Sp110*$^{-/-}$ lungs resembled those of wild-type B6 mice (Figure 1B) and harbored fewer bacteria
147 than the lungs of B6.*Sst1*^{S} mice, similar to both the B6 and *Sp110*$^{+/-}$ littermates (Figure 1C).
148 Likewise, the survival of infected *Sp110*$^{-/-}$ mice was indistinguishable from B6 mice, and mice
149 of both genotypes survived considerably longer than the B6.*Sst1*^{S} mice (Figure 1D). Thus,
150 despite the absence of *Sp110* from *Sst1*^{S} mice, our results indicate that the loss of *Sp110* is not
151 sufficient to replicate the susceptibility to *M. tuberculosis* associated with the *Sst1*^{S} locus.

152 ***Sp140*$^{-/-}$ mice are susceptible to bacterial infections.** Given that *Sp110* deficiency did not
153 phenocopy the susceptibility of *Sst1*^{S} mice, we asked whether any other genes found within the
154 *Sst1* locus differ in expression between B6 and B6.*Sst1*^{S} BMMs. We noted that a homolog of
155 *Sp110* called *Sp140* was also reduced in expression in B6.*Sst1*^{S} cells compared to B6 cells
156 (Figure 2A). Immunoblot confirmed that neither untreated nor IFN-γ treated BMMs from
157 B6.*Sst1*^{S} mice produce SP140 protein (Figure 2B). We therefore used CRISPR–Cas9 to generate
158 two independent lines of *Sp140*$^{-/-}$ mice on a pure B6 background (Figure 2 – figure supplement
159 1A-C). Our analysis focused primarily on line 1, which we found lacked expression of SP140
160 protein (Figure 2B) but retains the production of SP110 protein (Figure 2 – figure supplement
161 1D). Like *Sp110*$^{-/-}$ and *Sst1*^{S} mice, *Sp140*$^{-/-}$ mice are viable, fertile and born at the expected
162 Mendelian ratios. When infected with *M. tuberculosis*, however, *Sp140*$^{-/-}$ mice exhibited high
163 bacterial burdens in their lungs, similar to B6.*Sst1*^{S} mice and significantly greater than B6,
164 *Sp110*$^{-/-}$ or *Sp140*$^{+/-}$ littermate mice at day 28 post-infection (Figure 2C, Figure 2 – figure
165 supplement 1E). *Sp140*$^{-/-}$ lungs at 25 days post-infection with *M. tuberculosis* were more similar
166 to B6.*Sst1*^{s} lungs than to B6 or *Sp110*$^{-/-}$ lungs (Figure 2D, Figure 2 – figure supplement 2). The
167 increased susceptibility of *Sp140*$^{-/-}$ mice was accompanied by significant weight loss and
168 shortened survival upon infection with *M. tuberculosis*, again phenocopying the B6.*Sst1*^{S} mice
169 (Figure 2E-F). Both of the independent lines of *Sp140*$^{-/-}$ mice were similarly susceptible to *M.*
170 *tuberculosis* (Figure 2 – figure supplement 1E). We also found that both B6.*Sst1*^{S} and *Sp140*$^{-/-}$
171 mice were more susceptible to the intracellular Gram-negative bacterium *Legionella*
172 *pneumophila*, as compared to the B6 and *Sp110*$^{-/-}$ mice (Figure 2G).
173 An important caveat to the use of CRIPSR–Cas9 to generate *Sp140*$^{-/-}$ mice is the
174 presence of an unknown number of nearly identical *Sp140*-like genes in the *Sst1* locus and non-
175 localized chromosome 1 genome contigs (that presumably map to the adjacent HSR that remains
176 unassembled by the mouse genome project). It is possible that the guide RNA we used to disrupt
177 exon 3 of *Sp140* also disrupted these uncharacterized *Sp140*-like genes. However, it is not clear
178 if these uncharacterized *Sp140*-like genes give rise to functional proteins. Nevertheless, to
179 identify potential mutated off-target genes in our *Sp140*$^{-/-}$ mice, we amplified exons 2/3 of *Sp140*
180 and any potential paralogs from genomic DNA and from cDNA derived from *M. tuberculosis*-

181 infected lungs, and subjected the amplicons to deep sequencing (Figure 2 – figure supplement 3).
182 Although we found evidence for several edited *Sp140*-like exons in our *Sp140*$^{-/-}$ mice, only one
183 of these edited off-target genes was found to be detectably expressed from analysis of RNA-seq
184 data from *M. tuberculosis*-infected lungs, and this off-target appeared to be edited only in one of
185 our founder lines (Figure 2 – figure supplement 3B). Thus, mutation of *Sp140* itself is the most
186 parsimonious explanation for susceptibility of our *Sp140*$^{-/-}$ mice, a conclusion further supported
187 by complementation of the mutation in BMMs (see below, Figure 2 – figure supplement 4).
188 Collectively our results strongly suggest that the lack expression of *Sp140* in B6.*Sst1*^{S} mice
189 explains the broad susceptibility of these mice to bacterial infections.

190 **Enhanced type I IFN responses in *Sp140*$^{-/-}$ and B6.*Sst1*^{S} mice.** We and others previously
191 reported that TNFα induces higher levels of type I IFN-induced genes in *Sst1*^{S} BMMs as
192 compared to B6 BMMs (Bhattacharya et al., 2018; Ji et al., 2019). We also observed higher
193 levels of *Ifnb* transcripts in the lungs of B6.*Sst1*^{S} mice infected with *M. tuberculosis*, as
194 compared to infected B6 mice (Ji et al., 2019). Similar to B6.*Sst1*^{S} BMMs, *Sp140*$^{-/-}$ BMMs also
195 exhibited elevated expression of *Ifnb* and interferon-stimulated genes (ISGs) when stimulated
196 with TNFα (Figure 2 – figure supplement 4A). Importantly, we were also able to complement
197 the enhanced IFN phenotype of *Sp140*$^{-/-}$ BMMs by transducing *Sp140*$^{-/-}$ BMMs with a
198 retrovirus expressing a *Sp140* cDNA driven by a minimal CMV promoter (Figure 2 – figure
199 supplement 4B). Repression of *Ifnb* by overexpression of *Sp140* in *Sp140*$^{-/-}$ BMMs was
200 selective, as *Sp140* overexpression did not repress the transcription of *Tnfa* induced by TNFα
201 (Figure 2 – figure supplement 4B).
202 When infected with *M. tuberculosis*, the lungs of *Sp140*$^{-/-}$ and B6.*Sst1*^{S} mice also
203 exhibited higher levels of *Ifnb* transcript as compared to B6, *Sp110*$^{-/-}$ and *Sp140*$^{+/-}$ littermate
204 mice (Figure 3A). Likewise, during *L. pneumophila* infection, *Sp140*$^{-/-}$ mice expressed more
205 *Ifnb* in their lungs, as compared to B6 mice. Importantly, elevated *Ifnb* was evident at 48 hours
206 post-infection when there is no difference in bacterial burdens between the genotypes, and at 96
207 hours post-infection, when *Sp140*$^{-/-}$ mice have greater bacterial burdens (Figure 3B).

208 **Infected *Sp140*$^{-/-}$ and B6.*Sst1*^{S} lungs show similar gene expression patterns.** We used RNA
209 sequencing to analyze the global gene expression patterns in *M. tuberculosis*-infected lungs of
210 B6, *Sp110*$^{-/-}$, *Sp140*$^{-/-}$ and B6.*Sst1*^{S} mice at day 28 post-infection (Figure 4). Principal
211 component analysis revealed that while there is spread among individual samples, the expression
212 pattern of *Sp140*$^{-/-}$ and B6.*Sst1*^{S} lungs segregates from the expression pattern in B6 and *Sp110*$^{-/-}$
213 lungs along the PC1 axis (77% of variance) (Figure 4A). Euclidean distance analysis revealed a
214 similar pattern, with B6.*Sst1*^{S} and *Sp140*$^{-/-}$ mice clustering together, and away from B6 and
215 *Sp110*$^{-/-}$ mice (Figure 4B). At the time point analyzed (28 dpi), both *Sp140*$^{-/-}$ and B6.*Sst1*^{S} mice

216 exhibit higher bacterial burdens than B6 and *Sp110*$^{-/-}$ mice (Figure 2C). Thus, the similarity of
217 the gene expression profile of B6.*Sst1*^{S} and *Sp140*$^{-/-}$ lungs may merely reflect increased
218 inflammation in these lungs. Alternatively, the increased bacterial burdens may be due to a
219 similarly enhanced type I IFN response in these mice, which leads to secondary bacterial
220 outgrowth and inflammation. Therefore, we specifically compared the change in expression of
221 two subsets of genes: (1) hallmark inflammatory response pathway (Figure 4C) and (2) type I
222 interferon response genes (Figure 4D). This analysis revealed that B6.*Sst1*^{S} and *Sp140*$^{-/-}$ mice
223 not only show a similarly increased inflammatory gene signature, as expected, but in addition
224 showed a similarly increased type I IFN gene signature. Only 269 genes were significantly
225 differentially expressed (adjusted p-value <0.05) between *Sp140*$^{-/-}$ and B6.*Sst1*^{S} samples,
226 whereas 1520 genes were significantly differentially expressed between *Sp140*$^{-/-}$ and B6. Within
227 the 269 genes differentially expressed between *Sp140*$^{-/-}$ and B6.*Sst1*^{S}, 62 were immunoglobulin
228 genes and 62 were annotated as pseudogenes and most differences are only of modest
229 significance (Figure 4E). At present, we cannot explain these differences, but since these genes
230 are not linked to the *Sst1* locus, and since *Sp110*$^{-/-}$ mice did not exhibit similar changes, we
231 suspect these expression differences reflect background differences between the *Sst1*^{S} and
232 *Sp140*$^{-/-}$ strains. Interestingly, the gene most significantly differentially expressed between
233 B6.*Sst1*^{S} and *Sp140*$^{-/-}$ mice (i.e., with the smallest adjusted *p*-value) was *Sp110* (Figure 4E). This
234 result is expected, given that *Sp110* is not expressed in B6.*Sst1*^{S} but is retained in our *Sp140*$^{-/-}$
235 mice (Figure 2 – figure supplement 1D). Together, these results show that while they are not
236 identical, the transcriptomes of *Sp140*$^{-/-}$ and B6.*Sst1*^{S} mice greatly overlap during *M.*
237 *tuberculosis* infection, and importantly, both strains exhibit a similar type I IFN signature. Given
238 the susceptibility of B6.*Sst1*^{S} mice is due to overproduction of type I IFN (Ji et al., 2019), we
239 hypothesized that type I IFNs might also mediate the susceptibility of *Sp140*$^{-/-}$ mice.

240 **Susceptibility of *Sp140*$^{-/-}$ mice to bacterial infections is dependent on type I IFN signaling.**
241 To determine whether type I IFNs exacerbate *M. tuberculosis* infection of *Sp140*$^{-/-}$ mice, *M.*
242 *tuberculosis*-infected *Sp140*$^{-/-}$ mice were treated with a blocking antibody against IFNAR1.
243 Compared to mice that only received isotype control antibody, *Sp140*$^{-/-}$ mice that received the
244 anti-IFNAR1 antibody had reduced bacterial burdens in their lungs (Figure 5 – figure
245 supplement 1). We also generated *Sp140*$^{-/-}$*Ifnar*$^{-/-}$ double-deficient mice and infected them with
246 *M. tuberculosis* (Figure 5A-B). Loss of *Ifnar* protected *Sp140*$^{-/-}$ mice from weight loss (Figure
247 5A) and reduced bacterial burdens at day 25 post-infection, similar to those seen in B6 mice
248 (Figure 5B). Furthermore, *Sp140*$^{-/-}$*Ifnar*$^{-/-}$ mice were partially protected from *L. pneumophila*
249 infection, to a similar degree as B6.*Sst1*^{S}*Ifnar*$^{-/-}$ mice (Figure 5C-D). These results show that
250 similar to B6.*Sst1*^{S} mice, type I IFN signaling is responsible for the susceptibility of *Sp140*$^{-/-}$

251 mice to *M. tuberculosis*, and partially responsible for the susceptibility of *Sp140*$^{-/-}$ mice to *L.*
252 *pneumophila.*

253

254 **Discussion**

255 Humans and other vertebrates encounter diverse classes of pathogens, including viruses, bacteria,
256 fungi and parasites. In response, vertebrate immune systems have evolved stereotypical
257 responses appropriate for distinct pathogen types. For example, type I IFN-driven immunity is
258 generally critical for defense against viruses (Schneider et al., 2014; Stetson and Medzhitov,
259 2006), whereas type II IFN (IFN-γ)-driven immunity mediates resistance to intracellular
260 pathogens (Crisler and Lenz, 2018). Additionally, IL-1 is important for inducing neutrophil and
261 other responses against extracellular pathogens (Mantovani et al., 2019), and IL-4/-13 (Type 2
262 immunity) orchestrates responses to helminths and other parasites (Locksley, 1994). Thus, an
263 important question is how the immune system generates responses that are appropriate for
264 resistance to a specific pathogen while repressing inappropriate responses. The alternative
265 strategy of making all types of responses to all pathogens appears not to be employed, possibly
266 because it would be too energetically costly, or incur too much inflammatory damage to the host.
267 Although there is still much to be learned, it appears that negative feedback is essential to
268 enforce choices between possible types of immune responses. For example, IL-4 and IFN-γ have
269 long been appreciated to act as reciprocal negative antagonists of each other (Locksley, 1994). In
270 addition, anti-viral type I IFNs have long been appreciated to negatively regulate IFN-γ and IL-1-
271 driven anti-bacterial responses (Donovan et al., 2017; Moreira-Teixeira et al., 2018). Although
272 negative regulation of IFN-γ/IL-1 by type I IFN is likely beneficial to limit immunopathology
273 during viral infections, *Sst1*^{S} mice provide an example of how excessive or inappropriate
274 negative regulation by type I IFN can also be detrimental during bacterial infections (He et al.,
275 2013; Ji et al., 2019). In this study, we therefore sought to understand the molecular mechanisms
276 by which wild-type (*Sst1*^{R}) mice are able to restrain type I IFNs appropriately during bacterial
277 infections.

278 Although the *Sst1* locus was first described in 2005 (Pan et al., 2005), further genetic
279 analysis of the locus has been hindered by its extreme repetitiveness and the concomitant
280 difficulty in generating specific loss-of-function mutations in *Sst1*-linked genes. In particular, the
281 loss of *Sp110 (Ipr1)* has long been proposed to explain the susceptibility of *Sst1* mice to bacterial
282 infections. However, while we could confirm the loss of *Sp110* expression in *Sst1*^{S} mice, *Sp110*$^{-}$
283 $^{/-}$ mice were never generated and thus its essential role in host defense has been unclear. The
284 advent of CRIPSR/Cas9-based methods of genome engineering allowed us to generate *Sp110*$^{-/-}$

285 mice. Unexpectedly, we found *Sp110*$^{-/-}$ mice were fully resistant to *M. tuberculosis* infection,
286 and we thus conclude that lack of *Sp110* is not sufficient to explain the *Sst1*^{S} phenotype. An
287 important caveat of genetic studies of the *Sst1* locus is that generating specific gene knockouts is
288 still nearly impossible in this genetic region, even with CRISPR–Cas9. Indeed, the guide
289 sequence used to target exon 3 of *Sp110* also targets an unknown number of pseudogene copies
290 of *Sp110*-like genes located within the unassembled adjacent 'homogenously staining region' of
291 mouse chromosome 1. Thus, we expect that additional off-target mutations are likely present in
292 our *Sp110*$^{-/-}$ mutant mice. However, given that the *Sp110* pseudogenes are not known to be
293 expressed, we consider it unlikely that collateral mutations would affect our conclusions.
294 Moreover, any off-target mutations should differ among the three founder mice we analyzed and
295 are thus unlikely to explain the consistent resistant phenotype we observed in all three founders.
296 Lastly, since we were able to establish that all the founders at a minimum lack SP110 protein,
297 additional mutations would not affect our conclusion that *Sp110* is not essential for resistance to
298 *M. tuberculosis*.

299 Given that loss of *Sp110* was not sufficient to explain the susceptibility of *Sst1*^{S} mice to
300 bacterial infections, we considered other explanations. We found that *Sst1*^{S} mice also lack
301 expression of *Sp140*, an *Sst1*-linked homolog of *Sp110*. Our data suggest that deletion of *Sp140*
302 is sufficient to recapitulate the full *Sst1*^{S} phenotype including broad susceptibility to multiple
303 bacterial infections including *M. tuberculosis* and *L. pneumophila*. Importantly, the susceptibility
304 of *Sp140*$^{-/-}$ mice to bacterial infection correlates with an exacerbated type I IFN response, as is
305 also the case for *Sst1*^{S} mice. Likewise, as with *Sst1*^{S} mice, the susceptibility of *Sp140*$^{-/-}$ mice was
306 rescued by antibody blockade or genetic deletion of the type I IFN receptor (*Ifnar*). We therefore
307 conclude that loss of *Sp140* likely explains the *Sst1* phenotype. It remains possible that the
308 additional loss of *Sp110* in *Sst1*^{S} mice further exacerbates the *Sst1*^{S} phenotype as compared to
309 *Sp140*$^{-/-}$ mice. However, in our studies, we did not observe a consistent difference between *Sst1*^{S}
310 (i.e., *Sp110*$^{-/-}$*Sp140*$^{-/-}$) mice as compared to our *Sp140*$^{-/-}$ mice.

311 Another important caveat to our study is that it remains possible that our *Sp140*$^{-/-}$ mice
312 carry additional mutations that contribute to, or even fully explain, their observed phenotype.
313 This concern is somewhat ameliorated by our analysis of two independent *Sp140*$^{-/-}$ founders,
314 both of which exhibited susceptibility to *M. tuberculosis* (Figure 2 – figure supplement 1E). We
315 confirmed there is normal SP110 protein levels in the spleen of uninfected *Sp140*$^{-/-}$ mice, and
316 normal levels of *Sp110* and *Sp100* mRNA in the lungs of *M. tuberculosis*-infected mice. Thus,
317 collateral loss of SP100 or SP110 is unlikely to explain the phenotype of our *Sp140*$^{-/-}$ mice. To
318 address the possibility of mutations in unannotated SP-like genes, we used deep amplicon
319 sequencing of genomic DNA and cDNA from *Sp140*$^{-/-}$ mice. We confirmed that both founder

320 lines harbored distinct off-target mutations. Most of the identified off-target mutations are in
321 previously unidentified sequences that likely originate from *Sp140* paralogs within the unmapped
322 HSR, and may, like many of the HSR sequences, be pseudogenes. Most off-target mutated genes
323 also appear to be expressed at a far lower level than *Sp140* in lungs during *M. tuberculosis*
324 infection. In one of our *Sp140*$^{-/-}$ lines, we identified an off-target mutated *Sp140*-like paralog
325 that was expressed at detectable levels in the lungs of *M. tuberculosis*-infected mice. This
326 paralog was 100% identical to *Sp140* in the sequenced region and was only distinguished from
327 *Sp140* itself because it lacked the deletion that was introduced into the edited *Sp140* gene.
328 Importantly this previously undescribed *Sp140*-like expressed sequence was not mutated in our
329 second *Sp140*$^{-/-}$ line and is thus unlikely to explain resistance to *M. tuberculosis* infection. As an
330 alternative approach to confirm the phenotype of *Sp140*$^{-/-}$ mice is due to loss of *Sp140*, we
331 overexpressed *Sp140* in *Sp140*$^{-/-}$ BMMs. Crucially, we found *Sp140* complements aberrant
332 elevated *Ifnb1* transcription exhibited by *Sp140*$^{-/-}$ BMMs upon TNFα stimulation. Lastly, *Sp110*
333 and *Sp140* are the only two *Sst1*-linked genes that we were able to find to be differentially
334 expressed between B6 and B6.*Sst1*^{S} mice, and as discussed above, our genetic studies suggest
335 little role for the loss of *Sp110*. Thus, while it is formally possible that an edited *Sp140* homolog
336 that was not identified by our amplicon sequencing contributes to the susceptibility to bacterial
337 infection and elevated type I IFN in *Sp140*$^{-/-}$ mice, the most parsimonious explanation of our
338 data is that deficiency in *Sp140* accounts for the *Sst1*^{S} phenotype. We expect that future
339 mechanistic studies will be critical to further confirm this conclusion.

340 Because *Sp140* is inducible by IFN-γ, our results suggest the existence of a novel
341 feedback loop by which IFN-γ acts to repress the transcription of type I IFNs via SP140. This
342 feedback loop appears to be essential for host defense against diverse bacterial pathogens. A
343 major question that remains is how SP140 acts to repress the type I IFN response. SP140
344 contains DNA/chromatin-binding domains, such as SAND, PHD and Bromodomains, which
345 suggests the hypothesis that SP140 functions as a direct transcriptional repressor of type I IFN
346 genes. However, much more indirect mechanisms are also possible. Recent studies suggest that
347 hyper type I IFN responses in TNF-stimulated B6.*Sst1*^{s} BMMs derive from aberrant oxidative
348 stress that activates the kinase JNK and ultimately results in a non-resolving stress response that
349 promotes necrosis (Bhattacharya et al., 2020; Brownhill, 2020). Interestingly, mouse SP140
350 localizes to nuclear structures called PML bodies. PML bodies are implicated in a variety of cell
351 processes such as apoptosis, cell cycle, DNA damage response, senescence, and cell-intrinsic
352 antiviral responses (Scherer and Stamminger, 2016). Whether or not the repressive effects of
353 SP140 on type I IFN expression occur via the activity of PML bodies is an important outstanding
354 question. Another major question is whether or how the repression of type I IFNs by SP140 is

355 specific for bacterial infections and, if not, whether the presence of SP140 impairs anti-viral
356 immunity. Lastly, polymorphisms in human SP140 are associated with chronic lymphocytic
357 leukemia (CLL), Crohn's disease and multiple sclerosis (MS) (Franke et al., 2010; Jostins et al.,
358 2012; Karaky et al., 2018; Matesanz et al., 2015; Slager et al., 2013). Studies using siRNA and
359 shRNA-mediated knockdown have also implicated SP140 in the repression of lineage-
360 inappropriate genes in macrophages (Mehta et al., 2017). Our generation of *Sp140*$^{-/-}$ mice is
361 therefore important to permit future studies into these alternative roles of SP140.

362

363 **Materials and Methods**

364 **Mice.** All mice were specific pathogen-free, maintained under a 12-hr light-dark cycle (7AM to
365 7PM), and given a standard chow diet (Harlan irradiated laboratory animal diet) *ad libitum*. All
366 mice were sex and age-matched at 6-10 weeks old at the beginning of infections. C57BL/6J (B6)
367 and B6(Cg)-*Ifnar1tm1.2Ees*/J (*Ifnar*$^{-/-}$) were originally purchased from Jackson Laboratories
368 and subsequently bred at UC Berkeley. B6J.C3-*Sst* $^{C3HeB/FeJ}$Krmn mice (referred to as B6.*Sst1*^{S}
369 throughout) were from the colony of I. Kramnik at Boston University and then transferred to UC
370 Berkeley. CRISPR/Cas9 targeting was performed by pronuclear injection of Cas9 mRNA and
371 sgRNA into fertilized zygotes from colony-born C57BL/6J mice, essentially as described
372 previously (Wang et al., 2013). Founder mice were genotyped as described below, and founders
373 carrying *Sp140* mutations were bred one generation to C57BL/6J to separate modified *Sp140*
374 haplotypes. Homozygous lines were generated by interbreeding heterozygotes carrying matched
375 *Sp140* haplotypes. *Sp140*$^{-/-}$*Ifnar*$^{-/-}$ were generated by crossing the *Sp140*$^{-/-}$ and *Ifnar*$^{-/-}$ mice in-
376 house. All animals used in experiments were bred in-house unless otherwise noted in the figure
377 legends. All animal experiments complied with the regulatory standards of, and were approved
378 by, the University of California Berkeley Institutional Animal Care and Use Committee.

379 **Genotyping of *Sp110* alleles.** Exon 3 and the surrounding intronic regions were amplified by
380 PCR using the following primers (all 5' to 3'): Sp110 fwd, CTCTCCGCTCGGTGACTAC, and
381 rev, CTGCACATGTGACAAGGATCTC. The primer combinations were designed to
382 distinguish *Sp110* from other *Sp110*-like genes. Primers were used at 200nM in each 20µl
383 reaction with 1x Dreamtaq Green PCR Master Mix (Thermo Fisher Scientific). Cleaned PCR
384 products were diluted at 1:10 and sequenced using Sanger sequencing (Elim Biopharm).

385 **Genotyping of *Sp140* alleles.** Exon 3 and the surrounding intronic regions were amplified by
386 bracket PCR using the following primers (all 5′ to 3′): Sp140-1 fwd,
387 ACGAATAGCAAGCAGGAATGCT, and rev, GGTTCCGGCTGAGCACTTAT. The PCR
388 products are diluted at 1:10 and 2µl were used as template for the second PCR using the

389 following primers: Sp140-2 fwd, TGAGGACAGAACTCAGGGAG, and rev,
390 ACACGCCTTTAATCCCAGCATTT. The primer combinations were designed to distinguish
391 *Sp140* from other *Sp140*-like genes. Primers were used at 200nM in each 20µl reaction with 1x
392 Dreamtaq Green PCR Master Mix (Thermo Fisher Scientific). Cleaned PCR products were
393 diluted at 1:10 and sequenced using Sanger sequencing (Elim Biopharm). PCRs were performed
394 as described above for *Sp110* and sequenced using Sanger sequencing (Elim Biopharm).

395 ***Mycobacterium tuberculosis* infections.** *M. tuberculosis* strain Erdman (gift of S.A. Stanley)
396 was used for all infections. Frozen stocks of this wild-type strain were made from a single
397 culture and used for all experiments. Cultures for infection were grown in Middlebrook 7H9
398 liquid medium supplemented with 10% albumin-dextrose-saline, 0.4% glycerol and 0.05%
399 Tween-80 for five days at 37°C. Mice were aerosol infected using an inhalation exposure system
400 (Glas-Col, Terre Haute, IN). A total of 9 ml of diluted culture was loaded into the nebulizer
401 calibrated to deliver ~20 to 50 bacteria per mouse as confirmed by measurement of colony
402 forming units (CFUs) in the lungs 1 day following infection. Mice were sacrificed at various
403 days post-infection (as described in figure legends) to measure CFUs and RNA levels. All but
404 one lung lobe was homogenized in PBS plus 0.05% Tween-80, and serial dilutions were plated
405 on 7H11 plates supplemented with 10% oleic acid, albumin, dextrose, catalase (OADC) and
406 0.5% glycerol. CFUs were counted 21 days after plating. The remaining lobe was used for
407 histology or for RNA extraction. For histology, the sample was fixed in 10% formalin for at least
408 48 hours then stored in 70% ethanol. Samples were sent to Histowiz Inc for embedding in wax,
409 sectioning and staining with hematoxylin and eosin. For survival experiments, mice were
410 monitored for weight loss and were euthanized when they reached a humane endpoint as
411 determined by the University of California Berkeley Institutional Animal Care and Use
412 Committee.

413 ***Legionella pneumophila* infections.** Infections were performed using *L. pneumophila* strain
414 JR32 Δ*flaA* (gift of D.S. Zamboni) as previously described (Goncalves et al., 2019; Mascarenhas
415 et al., 2015). Briefly, frozen cultures were streaked out on to BCYE plates to obtain single
416 colonies. A single colony was chosen and streaked on to a new BCYE plate to obtain a 1cm by
417 1cm square bacterial lawn, and incubated for 2 days at 37°C. The patch was solubilized in
418 autoclaved MilliQ water and the optical density was measured at 600nm. Culture was diluted to
419 2.5 x10^6 bacteria/ml in sterile PBS. The mice were first anesthetized with ketamine and xylazine
420 (90 mg/kg and 5 mg/kg, respectively) by intraperitoneal injection then infected intranasally with
421 40 µL with PBS containing a final dilution of 1×10^5 bacteria per mouse. For enumerating of
422 CFU, the lungs were harvested and homogenized in 5 mL of autoclaved MilliQ water for 30
423 seconds, using a tissue homogenizer. Lung homogenates were diluted in autoclaved MilliQ water

424 and plated on BCYE agar plates. CFU was enumerated after plates were incubated for 4 days at
425 37°C.

426 **Bone marrow-derived macrophages (BMMs) and TNF-treatment**. Bone marrow was
427 harvested from mouse femurs and tibias, and cells were differentiated by culture on non-tissue
428 culture-treated plates in RPMI supplemented with supernatant from 3T3-MCSF cells (gift of B.
429 Beutler), 10% fetal bovine serum (FBS), 2mM glutamine, 100 U/ml streptomycin and 100 µg/ml
430 penicillin in a humidified incubator (37°C, 5%CO2). BMMs were harvested six days after
431 plating and frozen in 95% FBS and 5% DMSO. For *in vitro* experiments, BMMs were thawed
432 into media as described above for 4 hours in a humidified 37°C incubator. Adherent cells were
433 washed with PBS, counted and replated at $1.2x10^6$ ~ $1.5x10^6$ cells/well in a TC-treated 6-well
434 plate. Cells were treated with 10 ng/ml recombinant mouse TNFα (410-TRNC-010, R&D
435 systems) diluted in the media as described above.

436 **Quantitative/conventional RT-PCR**. Total RNA from BMMs was extracted using E.Z.N.A.
437 Total RNA Kit I (Omega Bio-tek) according to manufacturer specifications. Total RNA from
438 infected tissues was extracted by homogenizing in TRIzol reagent (Life technologies) then
439 mixing thoroughly with chloroform, both done under BSL3 conditions. Samples were then
440 removed from the BSL3 facility and transferred to fresh tubes under BSL2 conditions. Aqueous
441 phase was separated by centrifugation and RNA was further purified using the E.Z.N.A. Total
442 RNA Kit I (Omega Bio-tek). Equal amounts of RNA from each sample were treated with DNase
443 (RQ1, Promega) and cDNA was made using Superscript III (Invitrogen). Complementary cDNA
444 reactions were primed with poly(dT) for the measurement of mature transcripts. For experiments
445 with multiple time points, macrophage samples were frozen in the RLT buffer (Qiagen) and
446 infected tissue samples in RNA*later*™ solution (Invitrogen) and processed to RNA at the same
447 time. Quantitative PCR was performed using QuantiStudio 5 Real-Time PCR System (Applied
448 Biosystems) with Power Sybr Green PCR Master Mix (Thermo Fisher Scientific) according to
449 manufacturer specifications. Transcript levels were normalized to housekeeping genes *Rps17,*
450 *Actb* and *Oaz1* unless otherwise specified. The following primers were used in this study. *Rps17*
451 sense: CGCCATTATCCC CAGCAAG; *Rps17* antisense: TGTCGGGATCCACCTCAATG;
452 *Oaz1* sense: GTG GTG GCC TCT ACA TCG AG; *Oaz1* antisense: AGC AGA TGA AAA CGT
453 GGT CAG; *Actb* sense: CGC AGC CAC TGT CGA GTC; *Actb* antisense: CCT TCT GAC CCA
454 TTC CCA CC; *Ifnb* sense: GTCCTCAACTGCTCTCCACT; *Ifnb* antisense:
455 CCTGCAACCACCACTCATTC; *Gbp4* sense: TGAGTACCTGGAGAATGCCCT; *Gbp4*
456 antisense: TGGCCGAATTGGATGCTTGG; *Ifit3* sense: AGCCCACACCCAGCTTTT; *Ifit3*
457 antisense: CAGAGATTCCCGGTTGACCT. *Tnfa* sense: TCTTCTCATTCCTGCTTGTGG;
458 *Tnfa* antisense: GGTCTGGGCCATAGAACTGA. Conventional RT-PCR shown in Figure 2A

459 was done using the following primers. Sense: GTCCCTTGGAGTCTGTGTAGG; antisense:
460 CATCCTGGGGCTCTTGTCTTG.

461 **Immunoblot.** Samples were lysed in RIPA buffer with protease inhibitor cocktail (Roche) to
462 obtain total protein lysate and were clarified by spinning at ~16,000×*g* for 30 min at 4°C.
463 Clarified lysates were analyzed with Pierce BCA protein assay kit (Thermo Fisher Scientific)
464 according to manufacturer specification and diluted to the same concentration and denatured
465 with SDS-loading buffer. Samples were separated on NuPAGE Bis–Tris 4% to 12% gradient
466 gels (Thermo Fisher Scientific) following the manufacturer's protocol. Gels were transferred
467 onto ImmobilonFL PVDF membranes at 35 V for 90 min and blocked with Odyssey blocking
468 buffer (Li-Cor). Proteins were detected on a Li-Cor Odyssey Blot Imager using the following
469 primary and secondary antibodies. Rabbit anti-SP110 or SP140 serums were produced by
470 Covance and used at 1:1000 dilution. Hybridoma cells expressing monoclonal anti-SP110
471 antibody were a gift of I. Kramnik. Antibodies were produced in-house as previously described
472 (Ji et al., 2019) and used at 100 ng/ml. Alexa Fluor 680-conjugated secondary antibodies
473 (Invitrogen) were used at 0.4 mg/ml.

474 **RNA sequencing and analysis**. Total RNA was isolated as described above. Illumina-
475 compatible libraries were generated by the University of California, Berkeley, QB3 Vincent J.
476 Coates Genomics Sequencing Laboratory. PolyA selection was performed to deplete rRNA.
477 Libraries were constructed using Kapa Biosystem library preparation kits. The libraries were
478 multiplexed and sequenced using one flow cell on Novaseq 6000 (Illumina) as 50bp paired-end
479 reads. Base calling was performed using bcl2fastq2 v2.20. The sequences were aligned to mm10
480 genome using Kallisto v.0.46.0 using standard parameters (Pimentel et al., 2017) and analyzed
481 using Deseq2 (Love et al., 2014) and DEVis packages (Price et al., 2019). For Deseq2 and
482 DEVis analysis, all raw counts were incremented by 1 to avoid excluding genes due to division
483 by 0 in the normalization process.

484 **Antibody-mediated neutralization**. Mice were given anti-IFNAR1 antibody or isotype control
485 once every 2 days, starting 7 days post-infection. All treatments were delivered by
486 intraperitoneal injection. Mouse anti-mouse IFNAR1 (MAR1-5A3) and isotype control (GIR208,
487 mouse anti-human IFNGR-α chain) were purchased from Leinco Technologies Inc. For
488 injections antibody stocks were diluted in sterile PBS and each mouse received 500 μg per
489 injection.

490 **Amplicon sequencing and analysis.** Amplicons comprising the 5'intron of exon 3 of *Sp140* and
491 the end of exon 3 were amplified from crude DNA from ear clips of Sp140KO-1 mice (sense:
492 TCATATAACCCATAAATCCATCATGACA; antisense:

493 CCATTTAGGAAGAAGTGTTTTAGAGTCT) with PrimeStar PCR components (Takara,
494 R010b) for 18 cycles according to manufacturer specifications, then diluted 50-fold and
495 barcoded for an additional 18 cycles with Illumina-compatible sequencing adaptors. Amplicons
496 of *Sp140* exon 3 (sense: AATATCAAGAAACATGTAAGAACCTGGT; antisense:
497 CCATTTAGGAAGAAGTGTTTTAGAGTCT) and exon 2-3 (sense:
498 GCAGAAGTTTCAGGAATATCAAGAAACATGTAAG; antisense:
499 ACTTCTTCTGTACATTGCTGAGGATGT) were amplified from cDNA generated from lungs
500 infected with *M. tuberculosis* for 25 cycles with PrimeStar before barcoding. Libraries were
501 generated by the University of California, Berkeley, QB3 Vincent J. Coates Genomics
502 Sequencing Laboratory, and were multiplexed and sequenced on an Illumina Miseq platform
503 with v2 chemistry and 300 bp single-end reads for DNA amplicons, and Illumina Miseq Nano
504 platform with v3 chemistry for 300bp single end reads for cDNA amplicons. Reads were aligned
505 with Burrows-Wheeler Aligner (BWA-MEM) with default parameters (Li, *et al*, 2009; Li, 2013)
506 to chromosome 1 and non-localized genome contigs of the *Mus musculus* genome (assembly
507 mm10) as well as the *Sp140* gene and transcript X1(XM_030255396.1), converted to BAM files
508 with samtools (Li, 2009), and visualized in IGV 2.8. Subsets of reads were extracted from
509 alignment files using the Seqkit toolkit (Shen, 2016).

510 **Retroviral transduction of BMMs.** Self-inactivating pTMGP vector (SINV) with either a
511 minimal CMV promoter driving Sp140 or a minimal CMV promoter and 4 Gal4 binding sites
512 driving mNeonGreen, and the reporter mAmetrine driven by a PGK promoter were cloned using
513 Infusion (638910, Takara). pTGMP was a gift from Scott Lowe (Addgene plasmid # 32716).
514 Virus was harvested from GP-2 cells transfected with SINV vectors and VSV-G grown in
515 DMEM supplemented with 30% FBS and 2mM glutamine, 100 U/ml streptomycin and 100
516 μg/ml penicillin (adapted from protocols described in Schmidt *et al*, 2015). Harvested virus was
517 concentrated 100-fold by ultracentrifugation in RPMI before storage at -80 °C. Virus was thawed
518 and titrated on bone marrow to optimize transduction efficiency. Bone marrow was harvested as
519 described above and the entirety of the bone marrow was plated in a non-TC 15 cm plate. The
520 next day, bone marrow was harvested and transduced with SINV virus on plates coated with 10
521 $\mu g/cm^2$ Retronectin (T100, Takara) for 1.5-2 hrs at 650 xg and 37°C. After 2 days of additional
522 culture, media was replenished, then transduced bone marrow was cultured for 3 additional days
523 before sorting. Sorted transduced macrophages were stimulated with 5 ng/mL recombinant
524 murine IFN-γ (575304, Biolegend) 12-14 hours before stimulation with 10 ng/mL recombinant
525 TNFα as described above for 4 hours (FBS used in these experiments was from Omega, LOT
526 721017, CAT# FB-12). RNA isolation and RT-qPCR were performed as described above.

527 **Statistical analysis**. All data were analyzed with Mann-Whitney test unless otherwise noted.
528 Tests were run using GraphPad Prism 5. *, $p \leq 0.05$; **, $p \leq 0.01$; ***, $p \leq 0.001$. All error bars
529 are s.e. Figures show exact p values for $p > 0.0005$.

530 **Data accession.** RNA-seq data is available at GEO, accession number GSE166114. Amplicon
531 sequencing data is available at the SRA, BioProject accession number PRJNA698382.

532 **Acknowledgements:** We thank the Stanley and Cox laboratories for support with *M.*
533 *tuberculosis* experiments, L. Flores, P. Dietzen and R. Chavez for technical assistance, and
534 members of the Vance, Barton, Cox, Stanley, and Portnoy labs for advice and discussions.

535 **Author contributions:** Conceptualization–D.X.J., K.H.D., A.Y.L., R.E.V.; Methodology–
536 D.X.J., K.C.W., D.I.K., S.R.M., A.L., K.J.C., A.Y.L., D.S.Z.; Resources–I.K., D.A.P., R.E.V.;
537 Data curation–D.X.J.; Writing – original draft preparation–D.X.J., R.E.V.; Writing – review &
538 editing–D.X.J., K.C.W., D.I.K., K.H.D., R.E.V.; Supervision–D.A.P., K.H.D., R.E.V.; Funding
539 acquisition–D.A.P., K.H.D., R.E.V.

540 **Funding**: R.E.V. is supported by an Investigator Award from the Howard Hughes Medical
541 Institute. This work was also supported by NIH grants R37AI075039 (R.E.V.), P01AI066302
542 (R.E.V. and D.A.P.). R.E.V. and K.H.D. were Burroughs Wellcome Fund Investigators in the
543 Pathogenesis of Infectious Disease.

544 **Competing Interests**: R.E.V. consults for Ventus Therapeutics.

545 **Ethics Statement**: Animal studies were approved by the UC Berkeley Animal Care and Use
546 Committee.

547

548

549 **Figure Legends**

550 **Figure 1. *Sp110*$^{-/-}$ mice are not susceptible to *M. tuberculosis* infections.** (**A**) BMDMs were
551 treated with 10 U/ml of IFNγ for 24 hours and cells were lysed with RIPA buffer. Five μg of
552 total protein was loaded on each lane, and immunoblot was performed with respective antibodies
553 as shown. Molecular weight standards are shown on the left of each blot in kDa. Individual
554 membranes were imaged separately. Three independent lines of *Sp100*$^{-/-}$ mice were analyzed
555 (denoted lines 61, 65, and 71). (**B-D**), Lungs of mice infected with *M. tuberculosis* were stained
556 with hematoxylin and eosin (H&E) for histology (**B**), measured for CFU at 25 days post-
557 infection (Mann-Whitney test) (**C**) or, monitored for survival (**D**). All except B6 mice were bred
558 in-house, and combined results from the three independent *Sp110*$^{-/-}$ lines are shown.
559 Representative of 2 experiments (**B, D**); combined results of 3 infections (**C**). *, $P \leq 0.05$; **, P
560 ≤ 0.01; ***, $P \leq 0.005$.

561 **Figure 2. *Sp140*$^{-/-}$ mice are susceptible to bacterial pathogens.** (**A**) RT-PCR of cDNA from
562 BMMs of the indicated genotypes. Red arrow indicates band corresponding to a portion of
563 *Sp140*, verified by sequencing. (**B**) Immunoblot of lysates from *Sp140*$^{-/-}$ and WT BMMs treated
564 with 10 U/ml of recombinant mouse IFNγ for 24 hours. Equal amounts of protein were loaded
565 for immunoblot with anti-SP140 antibody. (**C-F**) Mice were infected with *M. tuberculosis* and
566 measured for lung CFU at 28 days post-infection (**C**) body weight over time (**E**), and survival
567 (**F**). Statistics in (**E**) shows comparison to B6 at day 28, and data are from 10 B6, 11 B6.Sst1s,
568 and *Sp110*$^{-/-}$, 14 *Sp140*$^{-/-}$, and 6 *Sp140*$^{+/-}$mice. (**D**) H&E staining of lungs at 25 days post-
569 infection with *M. tuberculosis*. (**G**) Mice were infected with *L. pneumophila* and lungs were
570 measured for CFU at 96 hours post-infection. All mice were bred in-house, *Sp140*$^{-/-}$ and
571 *Sp140*$^{+/-}$ were littermates (**C-F**). **C**, **E**, and **G** are combined results of two independent
572 infections. **A-D** shows representative analysis of one *Sp140*$^{-/-}$ line (line 1), whereas **F-G**
573 includes a mixture of both line 1 and 2. Results of infection of both lines with *M. tuberculosis* is
574 shown in Figure S2E. (**C, E, F, G**) Mann-Whitney test. *, $p \leq 0.05$; **, $p \leq 0.01$; ***, $p \leq 0.005$.

575 **Figure 3. *Sp140*$^{-/-}$ mice have elevated *Ifnb* transcripts during bacterial infection.** (**A**) Mice
576 were infected with *M. tuberculosis* and at 28 days post-infection lungs were processed for total
577 RNA, which were used for RT-qPCR. Combined results of 2 independent experiments. (**B**) Mice
578 were infected with *L. pneumophila* and RT-qPCR was performed on lungs collected at indicated
579 times. Combined results of 2 independent infections. All mice were bred in-house, *Sp140*$^{-/-}$ and
580 *Sp140*$^{+/-}$ were littermates. (**A-B**) Mann-Whitney test. *, $p \leq 0.05$; **, $p \leq 0.01$; ***, $p \leq 0.005$.

581 **Figure 4. Global gene expression analysis of *Sp110*$^{-/-}$, *Sp140*$^{-/-}$ and B6.*Sst1*^{S} lungs after *M.*
582 ***tuberculosis* infection.** (**A**) PCA or (**B**) Euclidean distance analysis of all the samples. (**C-D**)

583 heatmaps of gene expression in $\log_2$-fold change from B6. Genes shown are those significantly
584 different between *Sp140*$^{-/-}$ and B6: (**C**) GSEA Hallmark inflammatory response; and (**D**) GO
585 type I IFN response genes. (**E**) volcano plot comparing *Sp140*$^{-/-}$ to B6.*Sst1*^{S} expression. Dots in
586 red are 2-fold differentially expressed with adjusted *p*-value ≤ 0.05.

587 **Figure 5. Susceptibility of *Sp140*$^{-/-}$ to *M. tuberculosis* and *L. pneumophila* is dependent on**
588 **type I IFN signaling**. (**A-B**) mice were infected with *M. tuberculosis* and measured for body
589 weight (**A**) and bacterial burdens at day 25 (**B**). Statistics in **A** show comparison to B6; data are
590 from 9 B6, and 13 *Sp140*$^{-/-}$ and *Sp140*$^{-/-}$ *Ifnar*$^{-/-}$ mice. Combined results of 2 experiments. (**C-**
591 **D**) bacteria burden in *L. pneumophila*-infected mice at 96 hours. Combined results of 2
592 experiments. All mice were bred in-house (**A-B**, **D**); all but B6 were bred in-house (**C**). Mann-
593 Whitney test (**A-D**). *, $p \leq 0.05$; **, $p \leq 0.01$; ***, $p \leq 0.005$.

594 **Figure 1 – figure supplement 1. CRISPR–Cas9 targeting strategy for *Sp110*$^{-/-}$ mice.** (**A**)
595 Mouse *Sp110* gene. Guide RNA sequence for CRISPR–Cas9 targeting and protospacer-adjacent
596 motif (PAM) are indicated. (**B-D**) *Sp110* locus in wildtype (WT) and three independent lines.
597 Homozygotes of 2 lines identified by sequencing (**B-C**), and heterozygote of the 3rd line by PCR
598 products separated on an agarose gel (**D**). Arrow indicates the mutant band.

599 **Figure 2 – figure supplement 1. CRISPR–Cas9 targeting strategy for *Sp140*$^{-/-}$ and**
600 **validation of founders.** (**A**) Mouse *Sp140* gene. Guide RNA sequence for CRISPR–Cas9
601 targeting and protospacer-adjacent motif (PAM) are indicated. (**B-C**) *Sp140* locus in wildtype
602 (WT) and 2 independent founders of *Sp140*$^{-/-}$ validated by sequencing. (**D**) Immunoblot for
603 SP110 using BMMs from mice of the indicated genotypes. Intervening lanes have been removed
604 for clarity (indicated by line in the image). (**E**) *M. tuberculosis*-infected mice were harvested for
605 CFU at 25 days post-infection. Empty and filled triangles indicate the two independent lines of
606 *Sp140*$^{-/-}$ used in this infection. All mice were bred in-house and *Sp140*$^{+/-}$ were littermates with
607 *Sp140*$^{-/-}$ line 2. Mann-Whitney test, *, $p \leq 0.05$; **, $p \leq 0.01$; ***, $p \leq 0.005$.

608 **Figure 2 – figure supplement 2. Histology of lungs from B6, B6.*Sst1*^{s}, *Sp110*$^{-/-}$, *Sp140*$^{-/-}$**
609 **mice after infection with *M. tuberculosis.*** H&E staining of entire lung sections from mice of
610 indicated genotypes at 25 days post-infection with *M. tuberculosis.* Black squares denote
611 sections shown in Figure 2C. Each image represents a lung section from a different mouse.
612 Borders in background color have been added around each image. Scale bar applies to all
613 images.

614 **Figure 2 – figure supplement 3. Characterization of off-targets in *Sp140*$^{-/-}$ mice.** (**A**)
615 Schematic of amplicon sequencing strategy for *Sp140* and *Sp140* homologs. (B) Summary of
616 edited *Sp140* homologs from amplicon sequencing and RNA-seq analysis. SNPs are denoted

617 based on the *Sp140* X1 transcript. Expression level was roughly estimated from read counts.
618 Three B6 and 2 *Sp140*$^{-/-}$ mice from each founder line were used as biological replicates for
619 *Sp140* exon 2/3 amplicon sequencing from cDNA, 2 mice per genotype were used for *Sp140*
620 exon 3 amplicon sequencing from cDNA, and 1 mouse per genotype was used for *Sp140* exon 3
621 amplicon sequencing from DNA.

622 **Figure 2 – figure supplement 4. Complementation of hyper type I IFN responses in *Sp140*$^{-}$**
623 **$^{/-}$ BMMs.** (**A**) BMMs were left untreated or treated with TNF-α for 24 hours. Total RNA was
624 used for RT-qPCR. Averages of technical duplicates for one biological replicate are shown. Data
625 is representative of two independent experiments. (**B**) RT-qPCR of *Sp140*$^{-/-}$ BMMs transduced
626 with either control SINV-minCMV-GAL4-mNeonGreen (SINV-mNeonGreen) or SINV-
627 minCMV-Sp140 (SINV-Sp140), primed with 5 ng/mL IFN-γ for 14 hours and treated with 10
628 ng/mL TNF-α for 4 hours. *, $p \leq 0.05$ calculated with an unpaired t-test with Welch's
629 correction. Data are representative of two independent experiments.

630 **Figure 5 – figure supplement 1. Antibody blockade of IFNAR1 reduces bacterial burden in**
631 ***Sp140*$^{-/-}$ mice during *M. tuberculosis* infection.** Mice were infected with *M. tuberculosis* and
632 treated with either IFNAR1-blocking antibody or isotype control starting 7 days post-infection.
633 At 25 days post-infection lungs were harvested to enumerate CFU. Results of one experiment.
634 All mice were bred in-house. Mann-Whitney test, *, $p \leq 0.05$; **, $p \leq 0.01$; ***, $p \leq 0.005$.

635

636

637

638 **References**

639 Anderson, M.S., and Su, M.A. (2016). AIRE expands: new roles in immune tolerance and
640 beyond. Nat Rev Immunol *16*, 247-258.
641 Auerbuch, V., Brockstedt, D.G., Meyer-Morse, N., O'Riordan, M., and Portnoy, D.A. (2004).
642 Mice lacking the type I interferon receptor are resistant to Listeria monocytogenes. J Exp
643 Med *200*, 527-533.
644 Bhattacharya, B., Chattrerjee, S., Berland, R., Pichugin, A.V., Gao, Y., Connor, J., Ivanov, A.,
645 Yan, B.S., Kobzik, L., and Kramnik, I. (2018). Increased susceptibility to intracellular
646 bacteria and necrotic inflammation driven by a dysregulated macrophage response to
647 TNF. bioRxiv.
648 Bottomley, M.J., Collard, M.W., Huggenvik, J.I., Liu, Z., Gibson, T.J., and Sattler, M. (2001).
649 The SAND domain structure defines a novel DNA-binding fold in transcriptional
650 regulation. Nat Struct Biol *8*, 626-633.
651 Boxx, G.M., and Cheng, G. (2016). The Roles of Type I Interferon in Bacterial Infection. Cell
652 Host Microbe *19*, 760-769.
653 Boyartchuk, V., Rojas, M., Yan, B.S., Jobe, O., Hurt, N., Dorfman, D.M., Higgins, D.E.,
654 Dietrich, W.F., and Kramnik, I. (2004). The host resistance locus sst1 controls innate
655 immunity to Listeria monocytogenes infection in immunodeficient mice. J Immunol *173*,
656 5112-5120.
657 Carrero, J.A., Calderon, B., and Unanue, E.R. (2004). Type I interferon sensitizes lymphocytes
658 to apoptosis and reduces resistance to Listeria infection. J Exp Med *200*, 535-540.
659 Chang, S.Y., Chen, M.L., Lee, M.R., Liang, Y.C., Lu, T.P., Wang, J.Y., and Yan, B.S. (2018).
660 SP110 Polymorphisms Are Genetic Markers for Vulnerability to Latent and Active
661 Tuberculosis Infection in Taiwan. Dis Markers *2018*, 4687380.
662 Crisler, W.J., and Lenz, L.L. (2018). Crosstalk between type I and II interferons in regulation of
663 myeloid cell responses during bacterial infection. Curr Opin Immunol *54*, 35-41.
664 Donovan, M.L., Schultz, T.E., Duke, T.J., and Blumenthal, A. (2017). Type I Interferons in the
665 Pathogenesis of Tuberculosis: Molecular Drivers and Immunological Consequences.
666 Front Immunol *8*, 1633.
667 Dorhoi, A., Yeremeev, V., Nouailles, G., Weiner, J., 3rd, Jorg, S., Heinemann, E., Oberbeck-
668 Muller, D., Knaul, J.K., Vogelzang, A., Reece, S.T.*, et al.* (2014). Type I IFN signaling
669 triggers immunopathology in tuberculosis-susceptible mice by modulating lung
670 phagocyte dynamics. Eur J Immunol *44*, 2380-2393.
671 Fox, G.J., Sy, D.N., Nhung, N.V., Yu, B., Ellis, M.K., Van Hung, N., Cuong, N.K., Thi Lien, L.,
672 Marks, G.B., Saunders, B.M.*, et al.* (2014). Polymorphisms of SP110 are associated with
673 both pulmonary and extra-pulmonary tuberculosis among the Vietnamese. PLoS One *9*,
674 e99496.
675 Franke, A., McGovern, D.P., Barrett, J.C., Wang, K., Radford-Smith, G.L., Ahmad, T., Lees,
676 C.W., Balschun, T., Lee, J., Roberts, R.*, et al.* (2010). Genome-wide meta-analysis
677 increases to 71 the number of confirmed Crohn's disease susceptibility loci. Nat Genet
678 *42*, 1118-1125.
679 Goncalves, A.V., Margolis, S.R., Quirino, G.F.S., Mascarenhas, D.P.A., Rauch, I., Nichols,
680 R.D., Ansaldo, E., Fontana, M.F., Vance, R.E., and Zamboni, D.S. (2019). Gasdermin-D
681 and Caspase-7 are the key Caspase-1/8 substrates downstream of the NAIP5/NLRC4
682 inflammasome required for restriction of Legionella pneumophila. PLoS pathogens *15*,
683 e1007886.

He, X., Berland, R., Mekasha, S., Christensen, T.G., Alroy, J., Kramnik, I., and Ingalls, R.R. (2013). The sst1 resistance locus regulates evasion of type I interferon signaling by Chlamydia pneumoniae as a disease tolerance mechanism. PLoS Pathog *9*, e1003569.

Ji, D.X., Yamashiro, L.H., Chen, K.J., Mukaida, N., Kramnik, I., Darwin, K.H., and Vance, R.E. (2019). Type I interferon-driven susceptibility to Mycobacterium tuberculosis is mediated by IL-1Ra. Nat Microbiol *4*, 2128-2135.

Jostins, L., Ripke, S., Weersma, R.K., Duerr, R.H., McGovern, D.P., Hui, K.Y., Lee, J.C., Schumm, L.P., Sharma, Y., Anderson, C.A.*, et al.* (2012). Host-microbe interactions have shaped the genetic architecture of inflammatory bowel disease. Nature *491*, 119-124.

Karaky, M., Fedetz, M., Potenciano, V., Andres-Leon, E., Codina, A.E., Barrionuevo, C., Alcina, A., and Matesanz, F. (2018). SP140 regulates the expression of immune-related genes associated with multiple sclerosis and other autoimmune diseases by NF-kappaB inhibition. Hum Mol Genet *27*, 4012-4023.

Lei, X., Zhu, H., Zha, L., and Wang, Y. (2012). SP110 gene polymorphisms and tuberculosis susceptibility: a systematic review and meta-analysis based on 10 624 subjects. Infect Genet Evol *12*, 1473-1480.

Li H, Handsaker B, Wysoker A, Fennell T, Ruan J, Homer N, Marth G, Abecasis G, Durbin R; 1000 Genome Project Data Processing Subgroup. (2009). The Sequence Alignment/Map format and SAMtools. Bioinformatics 25(16):2078-9.

Locksley, R.M. (1994). Th2 cells: help for helminths. J Exp Med *179*, 1405-1407.

Love, M.I., Huber, W., and Anders, S. (2014). Moderated estimation of fold change and dispersion for RNA-seq data with DESeq2. Genome Biol *15*, 550.

Mantovani, A., Dinarello, C.A., Molgora, M., and Garlanda, C. (2019). Interleukin-1 and Related Cytokines in the Regulation of Inflammation and Immunity. Immunity *50*, 778-795.

Mascarenhas, D.P., Pereira, M.S., Manin, G.Z., Hori, J.I., and Zamboni, D.S. (2015). Interleukin 1 receptor-driven neutrophil recruitment accounts to MyD88-dependent pulmonary clearance of legionella pneumophila infection in vivo. J Infect Dis *211*, 322-330.

Matesanz, F., Potenciano, V., Fedetz, M., Ramos-Mozo, P., Abad-Grau Mdel, M., Karaky, M., Barrionuevo, C., Izquierdo, G., Ruiz-Pena, J.L., Garcia-Sanchez, M.I.*, et al.* (2015). A functional variant that affects exon-skipping and protein expression of SP140 as genetic mechanism predisposing to multiple sclerosis. Hum Mol Genet *24*, 5619-5627.

Mayer-Barber, K.D., Andrade, B.B., Oland, S.D., Amaral, E.P., Barber, D.L., Gonzales, J., Derrick, S.C., Shi, R., Kumar, N.P., Wei, W.*, et al.* (2014). Host-directed therapy of tuberculosis based on interleukin-1 and type I interferon crosstalk. Nature *511*, 99-103.

McNab, F., Mayer-Barber, K., Sher, A., Wack, A., and O'Garra, A. (2015). Type I interferons in infectious disease. Nat Rev Immunol *15*, 87-103.

Mehta, S., Cronkite, D.A., Basavappa, M., Saunders, T.L., Adiliaghdam, F., Amatullah, H., Morrison, S.A., Pagan, J.D., Anthony, R.M., Tonnerre, P.*, et al.* (2017). Maintenance of macrophage transcriptional programs and intestinal homeostasis by epigenetic reader SP140. Sci Immunol *2*.

Moreira-Teixeira, L., Mayer-Barber, K., Sher, A., and O'Garra, A. (2018). Type I interferons in tuberculosis: Foe and occasionally friend. J Exp Med *215*, 1273-1285.

O'Connell, R.M., Saha, S.K., Vaidya, S.A., Bruhn, K.W., Miranda, G.A., Zarnegar, B., Perry, A.K., Nguyen, B.O., Lane, T.F., Taniguchi, T.*, et al.* (2004). Type I interferon production enhances susceptibility to Listeria monocytogenes infection. J Exp Med *200*, 437-445.

729 Pan, H., Yan, B.S., Rojas, M., Shebzukhov, Y.V., Zhou, H., Kobzik, L., Higgins, D.E., Daly,
730 M.J., Bloom, B.R., and Kramnik, I. (2005). Ipr1 gene mediates innate immunity to
731 tuberculosis. Nature *434*, 767-772.
732 Perniola, R., and Musco, G. (2014). The biophysical and biochemical properties of the
733 autoimmune regulator (AIRE) protein. Biochim Biophys Acta *1842*, 326-337.
734 Pichugin, A.V., Yan, B.S., Sloutsky, A., Kobzik, L., and Kramnik, I. (2009). Dominant role of
735 the sst1 locus in pathogenesis of necrotizing lung granulomas during chronic tuberculosis
736 infection and reactivation in genetically resistant hosts. Am J Pathol *174*, 2190-2201.
737 Pilla-Moffett, D., Barber, M.F., Taylor, G.A., and Coers, J. (2016). Interferon-Inducible GTPases
738 in Host Resistance, Inflammation and Disease. J Mol Biol *428*, 3495-3513.
739 Pimentel, H., Bray, N.L., Puente, S., Melsted, P., and Pachter, L. (2017). Differential analysis of
740 RNA-seq incorporating quantification uncertainty. Nat Methods *14*, 687-690.
741 Png, E., Alisjahbana, B., Sahiratmadja, E., Marzuki, S., Nelwan, R., Adnan, I., van de Vosse, E.,
742 Hibberd, M., van Crevel, R., Ottenhoff, T.H.*, et al.* (2012). Polymorphisms in SP110 are
743 not associated with pulmonary tuberculosis in Indonesians. Infect Genet Evol *12*, 1319-
744 1323.
745 Price, A., Caciula, A., Guo, C., Lee, B., Morrison, J., Rasmussen, A., Lipkin, W.I., and Jain, K.
746 (2019). DEvis: an R package for aggregation and visualization of differential expression
747 data. BMC Bioinformatics *20*, 110.
748 Rayamajhi, M., Humann, J., Penheiter, K., Andreasen, K., and Lenz, L.L. (2010). Induction of
749 IFN-alphabeta enables Listeria monocytogenes to suppress macrophage activation by
750 IFN-gamma. J Exp Med *207*, 327-337.
751 Roscioli, T., Cliffe, S.T., Bloch, D.B., Bell, C.G., Mullan, G., Taylor, P.J., Sarris, M., Wang, J.,
752 Donald, J.A., Kirk, E.P.*, et al.* (2006). Mutations in the gene encoding the PML nuclear
753 body protein Sp110 are associated with immunodeficiency and hepatic veno-occlusive
754 disease. Nat Genet *38*, 620-622.
755 Scherer, M., and Stamminger, T. (2016). Emerging Role of PML Nuclear Bodies in Innate
756 Immune Signaling. J Virol *90*, 5850-5854.
757 Schneider, W.M., Chevillotte, M.D., and Rice, C.M. (2014). Interferon-stimulated genes: a
758 complex web of host defenses. Annu Rev Immunol *32*, 513-545.
759 Slager, S.L., Caporaso, N.E., de Sanjose, S., and Goldin, L.R. (2013). Genetic susceptibility to
760 chronic lymphocytic leukemia. Semin Hematol *50*, 296-302.
761 Stetson, D.B., and Medzhitov, R. (2006). Type I interferons in host defense. Immunity *25*, 373-
762 381.
763 Thye, T., Browne, E.N., Chinbuah, M.A., Gyapong, J., Osei, I., Owusu-Dabo, E., Niemann, S.,
764 Rusch-Gerdes, S., Horstmann, R.D., and Meyer, C.G. (2006). No associations of human
765 pulmonary tuberculosis with Sp110 variants. J Med Genet *43*, e32.
766 Tosh, K., Campbell, S.J., Fielding, K., Sillah, J., Bah, B., Gustafson, P., Manneh, K., Lisse, I.,
767 Sirugo, G., Bennett, S.*, et al.* (2006). Variants in the SP110 gene are associated with
768 genetic susceptibility to tuberculosis in West Africa. Proc Natl Acad Sci U S A *103*,
769 10364-10368.
770 Wang, H., Yang, H., Shivalila, C.S., Dawlaty, M.M., Cheng, A.W., Zhang, F., and Jaenisch, R.
771 (2013). One-step generation of mice carrying mutations in multiple genes by
772 CRISPR/Cas-mediated genome engineering. Cell *153*, 910-918.

773 Weichenhan, D., Kunze, B., Winking, H., van Geel, M., Osoegawa, K., de Jong, P.J., and Traut,
774 W. (2001). Source and component genes of a 6-200 Mb gene cluster in the house mouse.
775 Mamm Genome *12*, 590-594.
776 Zhang, S., Wang, X.B., Han, Y.D., Wang, C., Zhou, Y., and Zheng, F. (2017). Certain
777 Polymorphisms in SP110 Gene Confer Susceptibility to Tuberculosis: A Comprehensive
778 Review and Updated Meta-Analysis. Yonsei Med J *58*, 165-173.
779

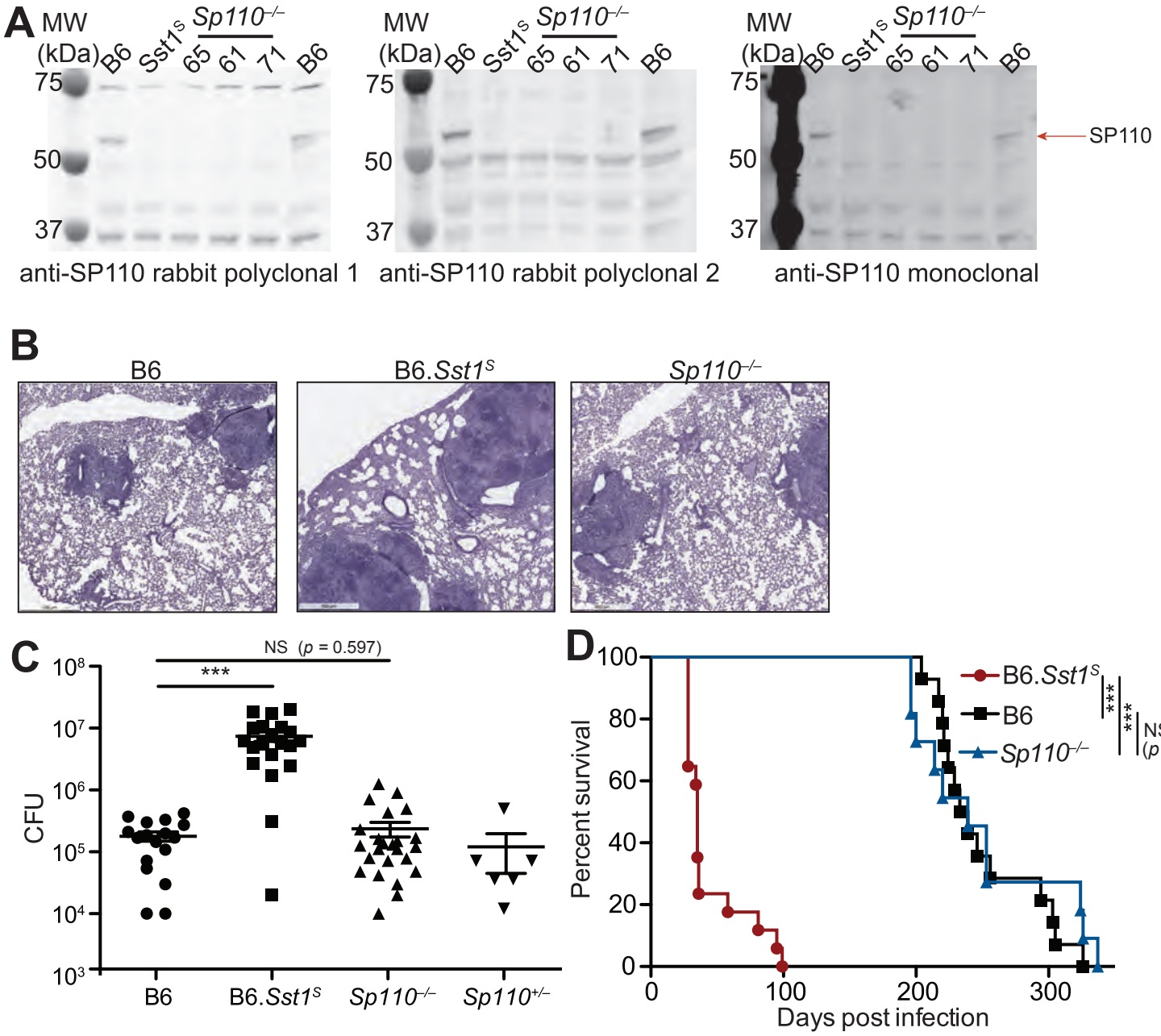

Figure 1. *Sp110*$^{-/-}$ mice are not susceptible to *M. tuberculosis* infections. (**A**) BMDMs were treated with 10 U/ml of IFNγ for 24 hours and cells were lysed with RIPA buffer. Five µg of total protein was loaded on each lane, and immunoblot was performed with respective antibodies as shown. Molecular weight standards are shown on the left of each blot in kDa. Individual membranes were imaged separately. Three independent lines of *Sp100*$^{-/-}$ mice were analyzed (denoted lines 61, 65, and 71). (**B**-**D**), Lungs of mice infected with *M. tuberculosis* were stained with hematoxylin and eosin (H&E) for histology (**B**), measured for CFU at 25 days post-infection (Mann-Whitney test) (**C**) or, monitored for survival (**D**). All except B6 mice were bred in-house, and combined results from the three independent *Sp110*$^{-/-}$ lines are shown. Representative of 2 experiments (**B**, **D**); combined results of 3 infections (**C**). *, $p \leq 0.05$; **, $p \leq 0.01$; ***, $p \leq 0.005$.

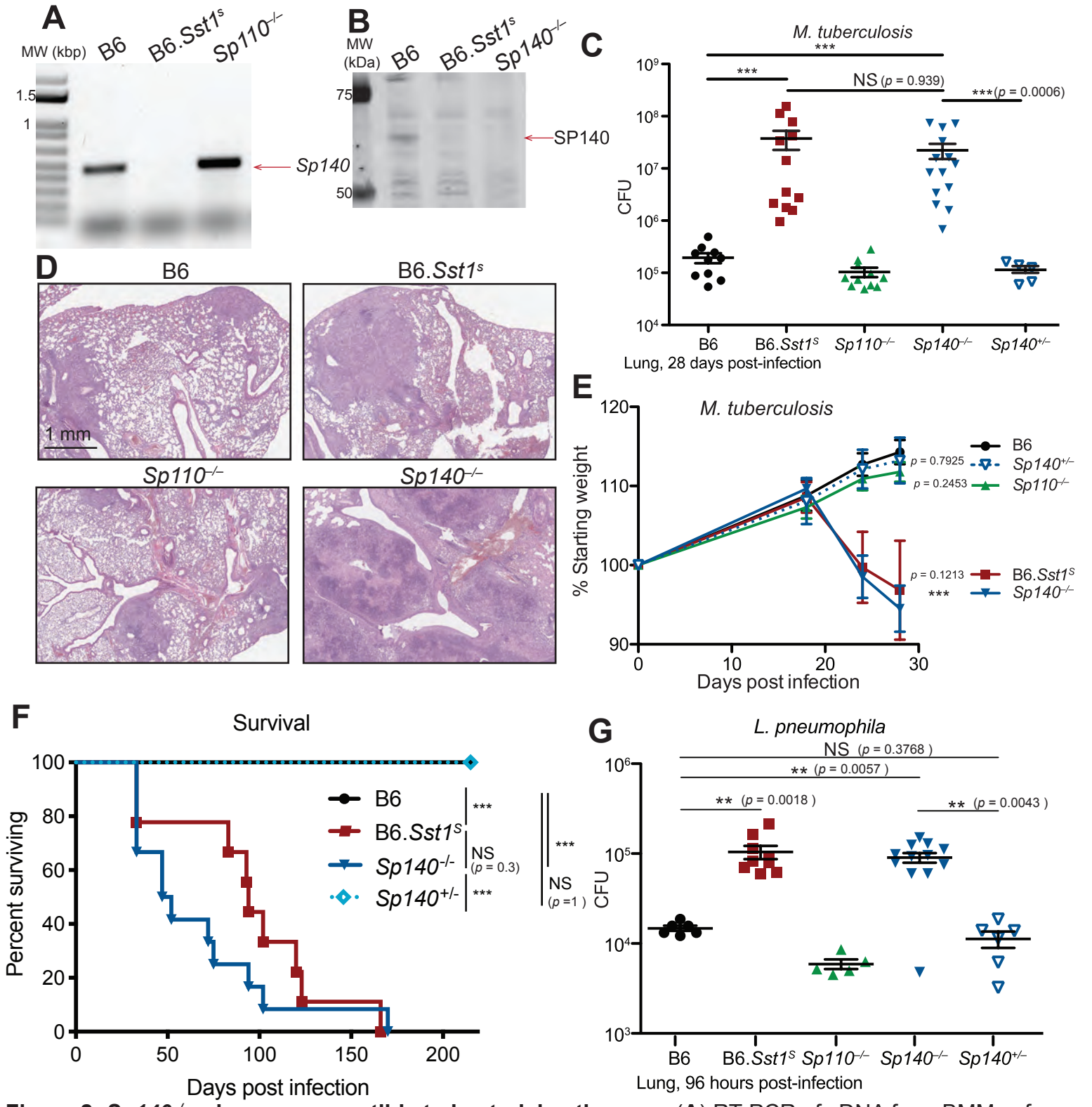

Figure 2. *Sp140*$^{-/-}$ mice are susceptible to bacterial pathogens. (**A**) RT-PCR of cDNA from BMMs of the indicated genotypes. Red arrow indicates band corresponding to a portion of Sp140, verified by sequencing. (**B**) Immunoblot of lysates from *Sp140*$^{-/-}$ and wildtype BMMs treated with 10 U/ml of recombinant mouse IFNγ for 24 hours. Equal amounts of protein were loaded for immunoblot with anti-SP140 antibody. (**C-F**) Mice were infected with *M. tuberculosis* and measured for lung CFU at 28 days post-infection (**C**), body weight over time (**E**), and survival (**F**). Statistics in (**E**) shows comparison to B6 at day 28, and data are from 10 B6, 11 B6.*Sst1*^{s} and *Sp110*$^{-/-}$, 14 *Sp140*$^{-/-}$, and 6 *Sp140*$^{+/-}$ mice. (**D**) H&E staining of lungs at 25 days post-infection with *M. tuberculosis*. (**G**) Mice were infected with *L. pneumophila* and lungs were measured for CFU at 96 hours post-infection. All mice were bred inhouse, and *Sp140*$^{-/-}$ and *Sp140*$^{+/-}$ were littermates (**C-G**). **C**, **E**, and **G** are combined results of two independent infections. **A-E** shows representative analysis of one *Sp140*$^{-/-}$ line (line 1), whereas **F-G** includes a mixture of both line 1 and 2. (**C**, **E**, **F**, **G**) Mann-Whitney test. *, $p \leq 0.05$; **, $p \leq 0.01$; ***, $p \leq 0.005$.

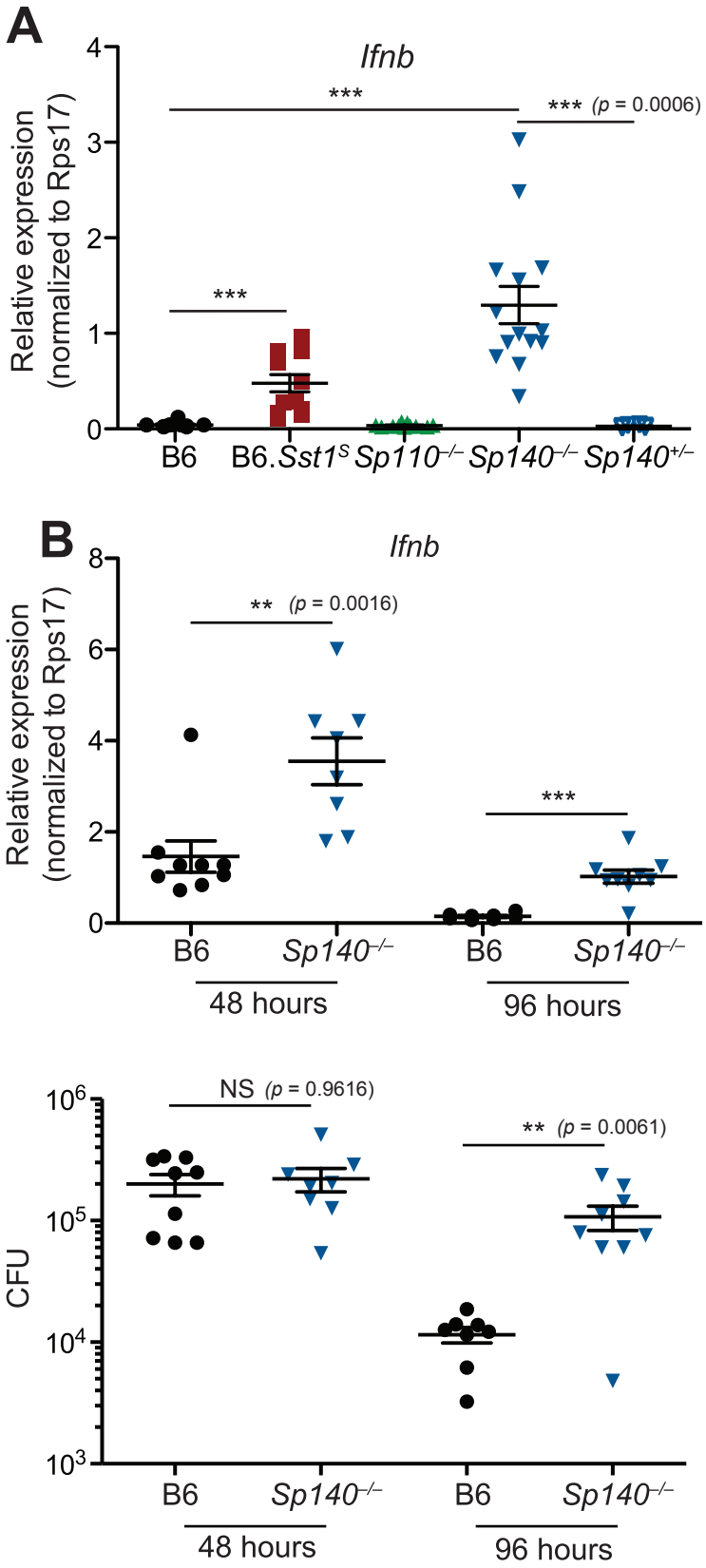

Figure 3. *Sp140*$^{-/-}$ mice have elevated *Ifnb* transcripts during bacterial infection. (**A**) Mice were infected with *M. tuberculosis* and at 28 days post-infection lungs were processed for total RNA, which were used for RT-qPCR. Combined results of 2 independent experiments. (**B**) Mice were infected with *L. pneumophila* and RT-qPCR was performed on lungs collected at indicated times. Combined results of 2 independent infections. All mice were bred in-house, *Sp140*$^{-/-}$ and *Sp140*$^{+/-}$ were littermates. (**A**-**B**) Mann-Whitney test. *, $p \leq 0.05$; **, $p \leq 0.01$; ***, $p \leq 0.005$.

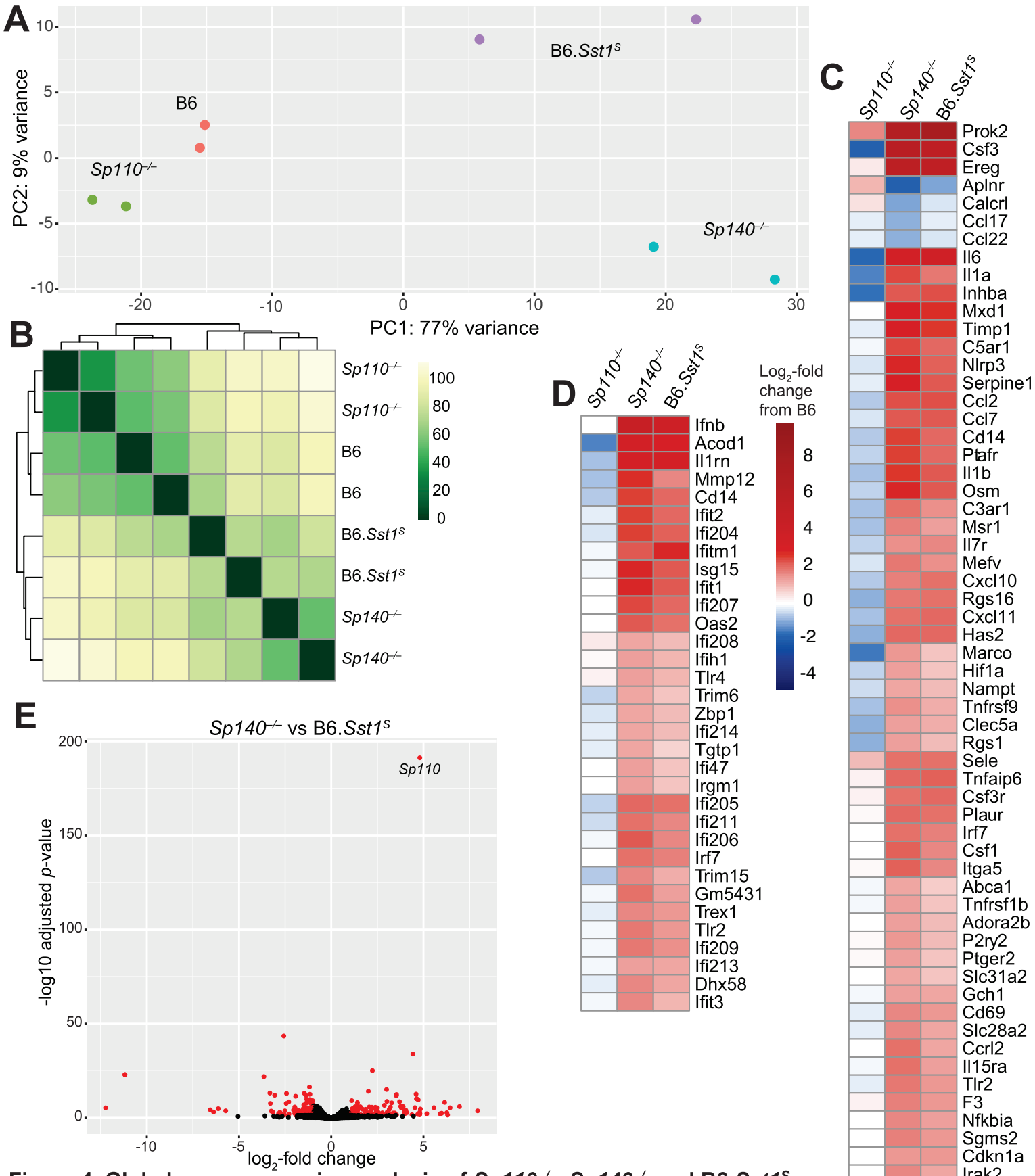

Figure 4. Global gene expression analysis of *Sp110*$^{-/-}$, *Sp140*$^{-/-}$ and B6.*Sst1*^{S} lungs after *M. tuberculosis* infection. (**A**) PCA or (**B**) Euclidean distance analysis of all the samples. (**C-D**) heatmaps of gene expression in $\log_2$-fold change from B6. Genes shown are those significantly different between *Sp140*$^{-/-}$ and B6 (**C**) GSEA Hallmark inflammatory response; and (**D**) GO type I IFN genes response genes. (**E**) volcano plot comparing *Sp140*$^{-/-}$ to B6.*Sst1*^{S} expression. Dots in red are 2-fold differentially expressed with adjusted *p*-value ≤ 0.05.

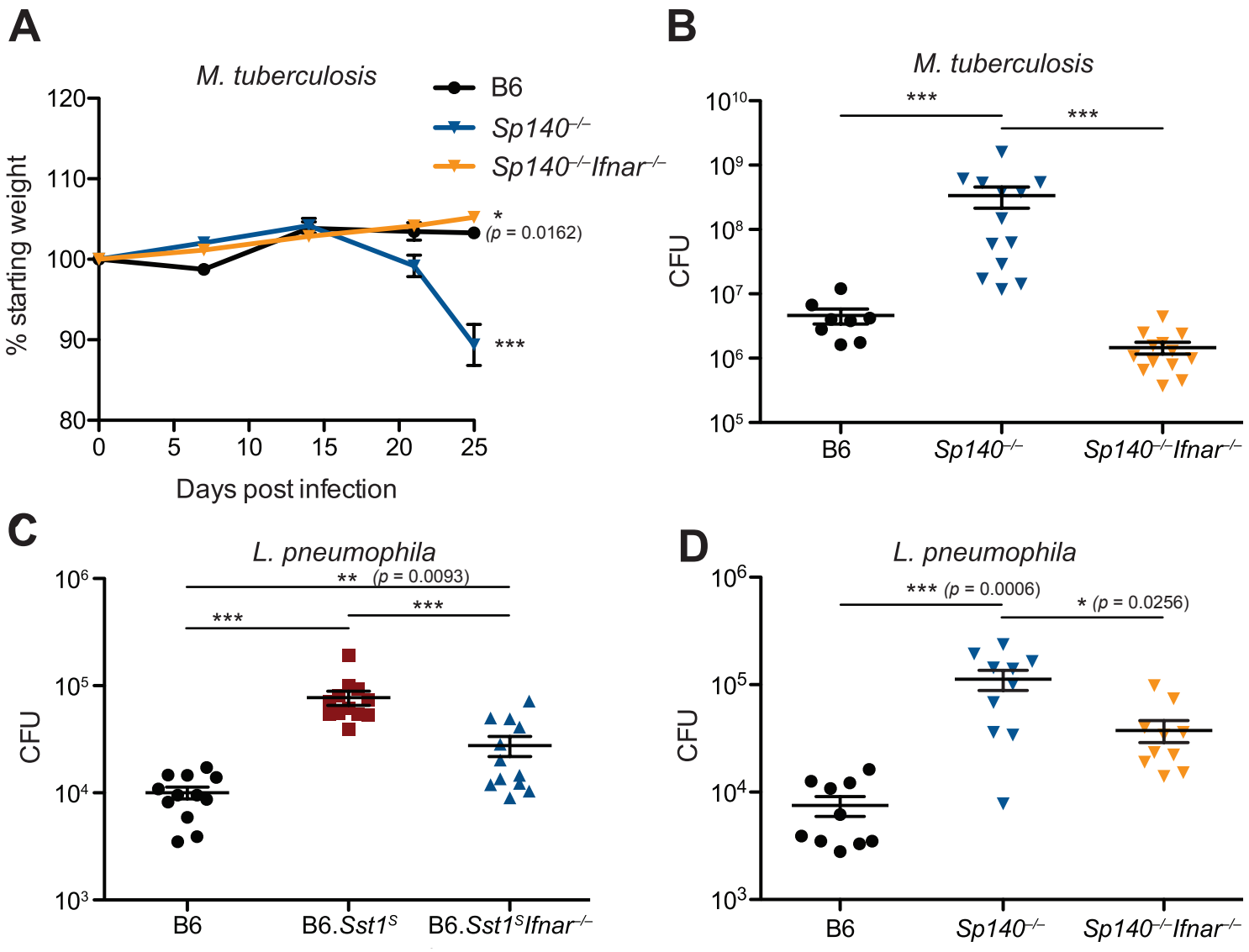

Figure 5. Susceptibility of *Sp140*$^{-/-}$ to *M. tuberculosis* and *L. pneumophila* is dependent on type I IFN signaling. (**A**-**B**) Mice were infected with *M. tuberculosis* and measured for body weight (**A**) and bacterial burdens at day 25 (**B**). Statistics in **A** show comparison to B6; data are from 9 B6, and 13 *Sp140*$^{-/-}$ and *Sp140*$^{-/-}$ *Ifnar*$^{-/-}$ mice. Combined results of 2 experiments. (**C**-**D**) bacteria burden in *L. pneumophila*-infected mice at 96 hours. Combined results of 2 experiments. All mice were bred in-house (**A**-**B**, **D**); all but B6 were bred in-house (**C**). Mann-Whitney test (**A**-**D**). *, $p \leq 0.05$; **, $p \leq 0.01$; ***, $p \leq 0.005$.

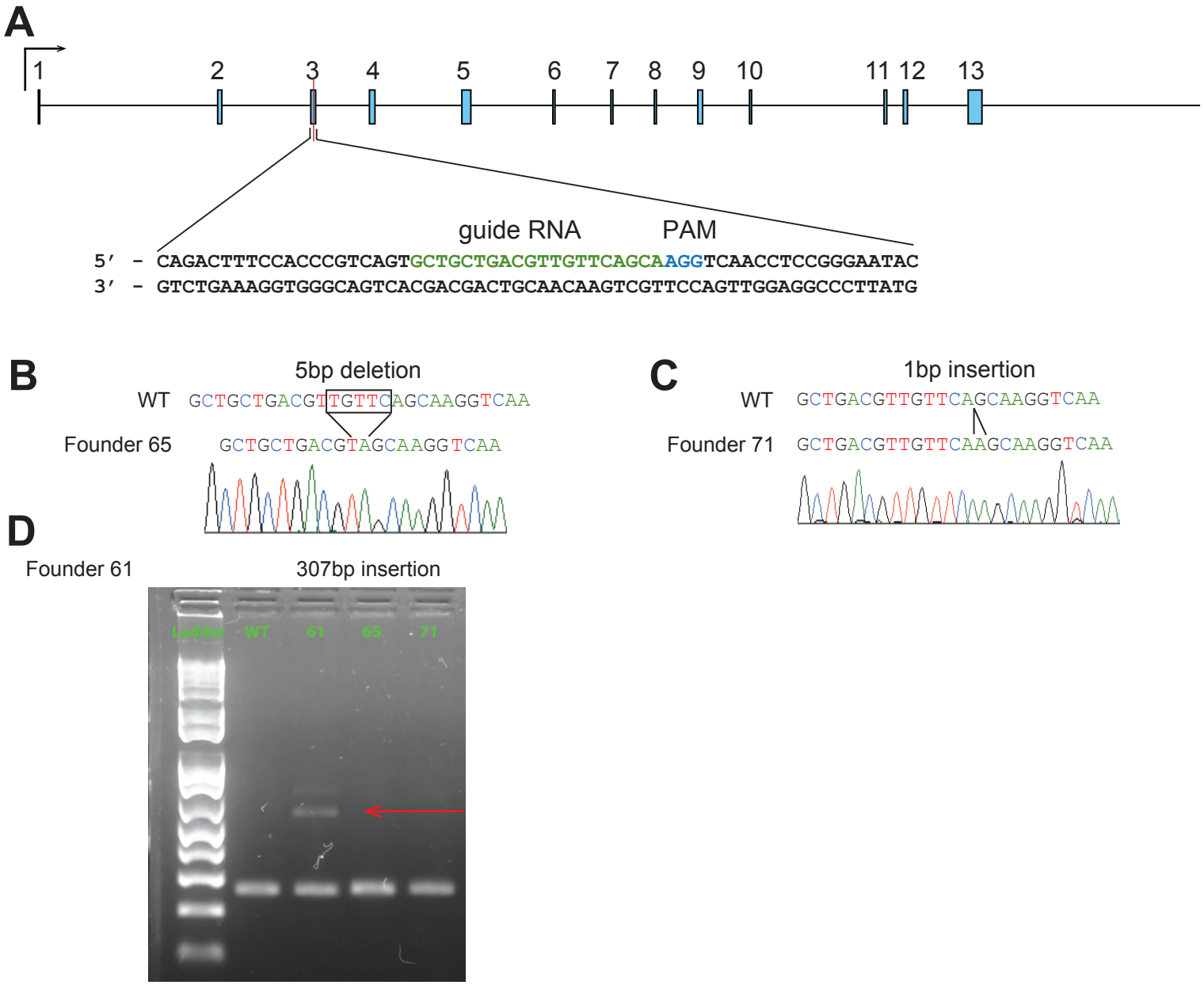

Figure 1– figure supplement 1. CRISPR–Cas9 targeting strategy for *Sp110*$^{-/-}$ mice. (**A**) Mouse *Sp110* gene. Guide RNA sequence for CRISPR–Cas9 targeting and protospacer-adjacent motif (PAM) are indicated. (**B**-**D**) *Sp110* locus in wildtype (WT) and three independent lines. Homozygotes of 2 lines identified by sequencing (**B**-**C**), and heterozygote of the 3rd line by PCR products separated on an agarose gel (**D**). Arrow indicates the mutant band.

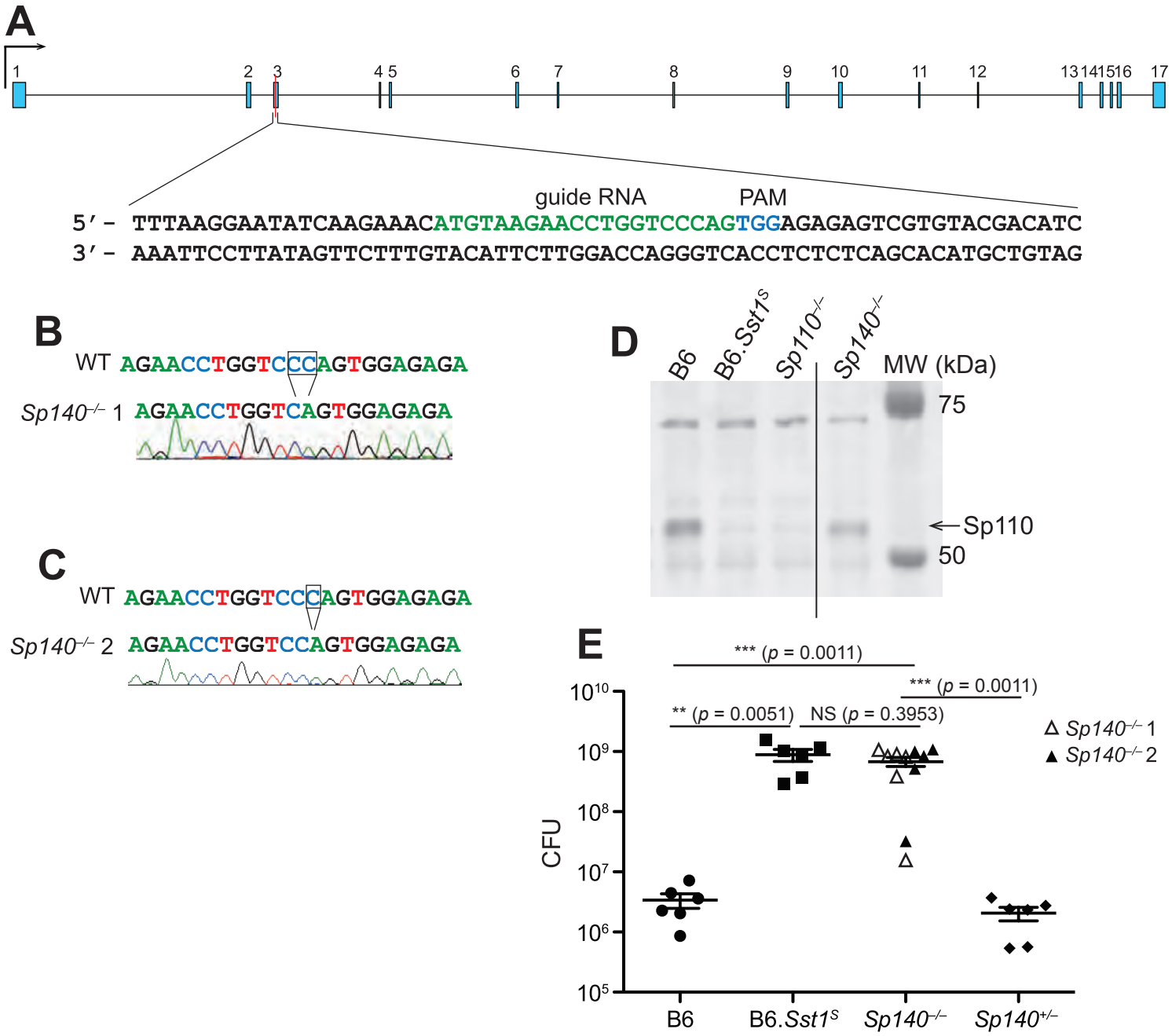

Figure 2 – figure supplement 1. CRISPR–Cas9 targeting strategy for *Sp140*$^{-/-}$ and validation of founders. (**A**) Mouse *Sp140* gene. Guide RNA sequence for CRISPR–Cas9 targeting and protospacer-adjacent motif (PAM) are indicated. (**B**-**C**) *Sp140* locus in wildtype (WT) and 2 independent founders of *Sp140*$^{-/-}$ validated by sequencing. (**D**) Immunoblot for SP110 using BMMs from mice of the indicated genotypes. Intervening lanes have been removed for clarity (indicated by line in the image). (**E**) *M. tuberculosis*-infected mice were harvested for CFU at 25 days post-infection. Empty and filled triangles indicate the two independent lines of *Sp140*$^{-/-}$ used in this infection. All mice were bred in-house and *Sp140*$^{+/-}$ were littermates with *Sp140*$^{-/-}$ line 2. Mann-Whitney test, *, $p \leq 0.05$; **, $p \leq 0.01$; ***, $p \leq 0.005$.

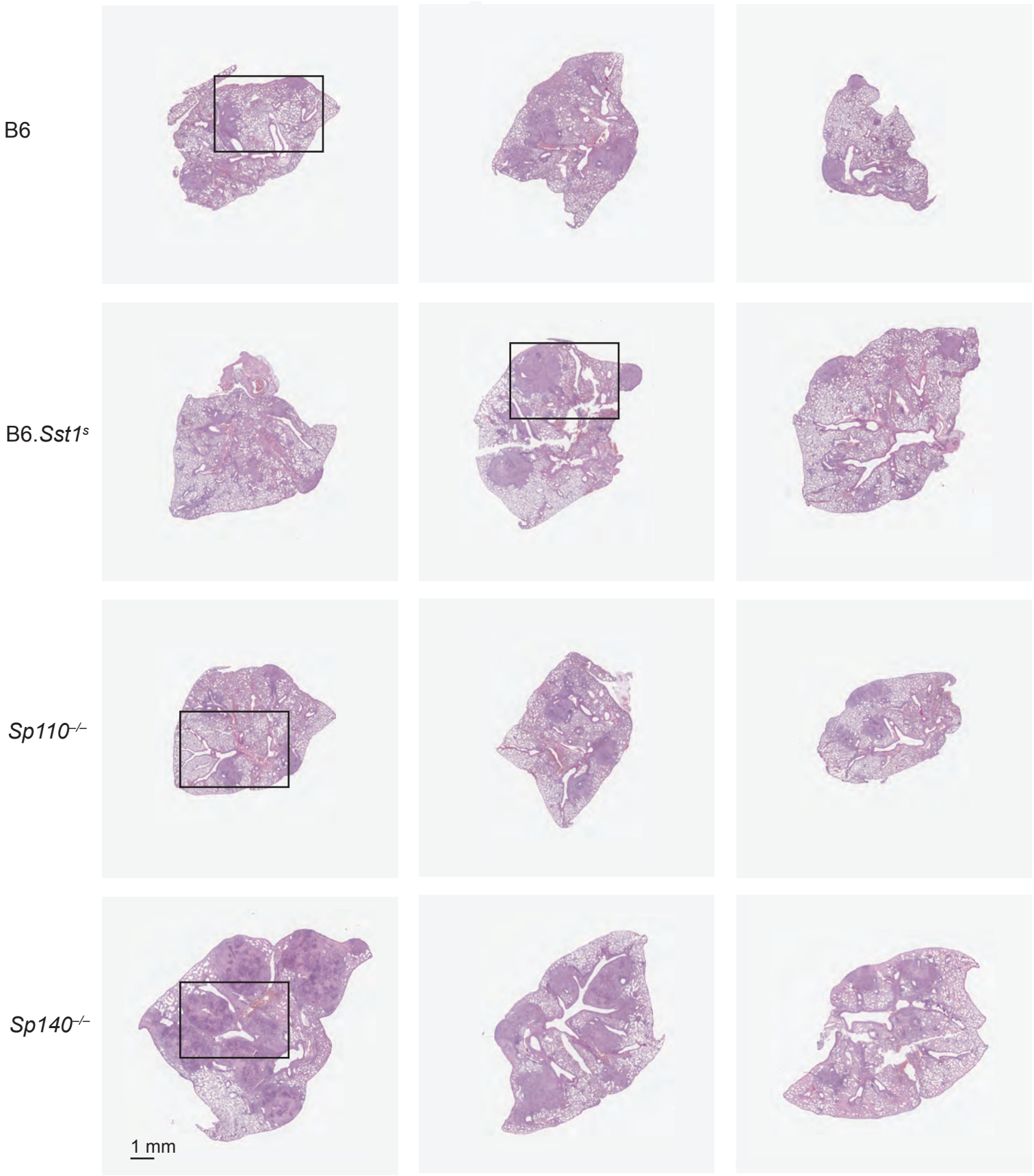

Figure 2 – figure supplement 2. Histology of B6, B6.*Sst1*^{s}, *Sp110*$^{-/-}$, *Sp140*$^{-/-}$ lungs infected with *M. tuberculosis.* H&E staining of entire lung sections from mice of indicated genotypes at 25 days post-infection with *M. tuberculosis.* Black squares denote sections shown in Figure 2C. Each image represents a lung section from a different mouse. Borders in background color have been added around each image. Scale bar applies to all images.

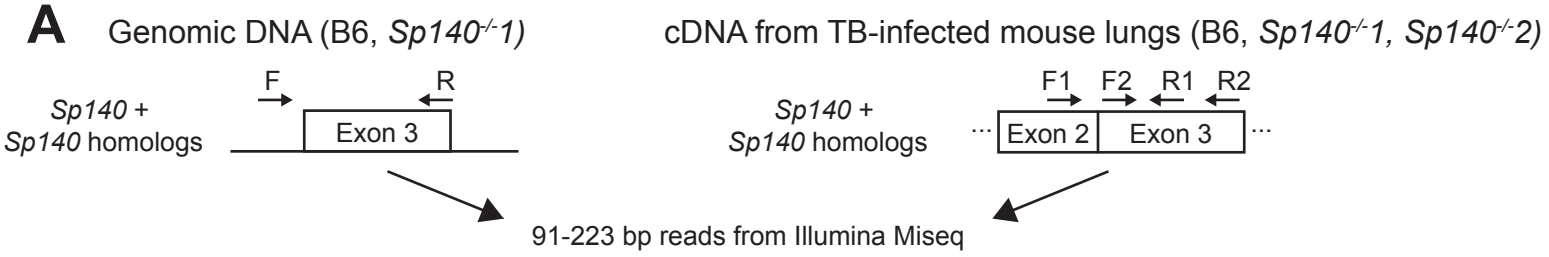

B Summary of edited *Sp140* homologs in *Sp140*$^{-/-}$ mice

Name	Dataset	Distinguishing SNPs from *Sp140* mRNA	Edited in *Sp140*$^{-/-}$*1*?	Edited in *Sp140*$^{-/-}$*2*?	Estimated level of expression in TB-infected lungs
LOC100041057	*Sp140* exon 3 amplicons, DNA (*Sp140*$^{-/-}$*1* and B6 only)	G at 1483, T at 1513	Yes	Unknown (not expressed)	None
Sp140 homolog 1	*Sp140* exon 3 amplicons, DNA (*Sp140*$^{-/-}$*1* and B6 only)	T at 1482, G at 1483	Yes	Unknown (not expressed)	None
Sp140 homolog 2	*Sp140* exon 2 and 3 amplicons, cDNA; RNA-seq of TB-infected lungs	None	Yes	No	Expressed
Sp140 homolog 3	*Sp140* exon 3 amplicons, cDNA	T at 1462	Yes	Yes	Very low (not detectable by RNA-seq)
Sp140 homolog 4	*Sp140* exon 3 amplicons, cDNA	T at 1500	Yes	Yes	Very low (not detectable by RNA-seq)

Figure 2 – figure supplement 3. Characterization of off-targets in *Sp140*$^{-/-}$ mice. (**A**) Schematic of amplicon sequencing strategy for *Sp140* and *Sp140* homologs. (**B**) Summary of edited *Sp140* homologs from amplicon sequencing and RNA-seq analysis. SNPs are denoted based on the *Sp140* X1 transcript. Expression level was roughly estimated from read counts. Two mice per genotype were used as biological replicates for amplicon sequencing for cDNA, and one mouse per genotype was used for amplicon sequencing from DNA.

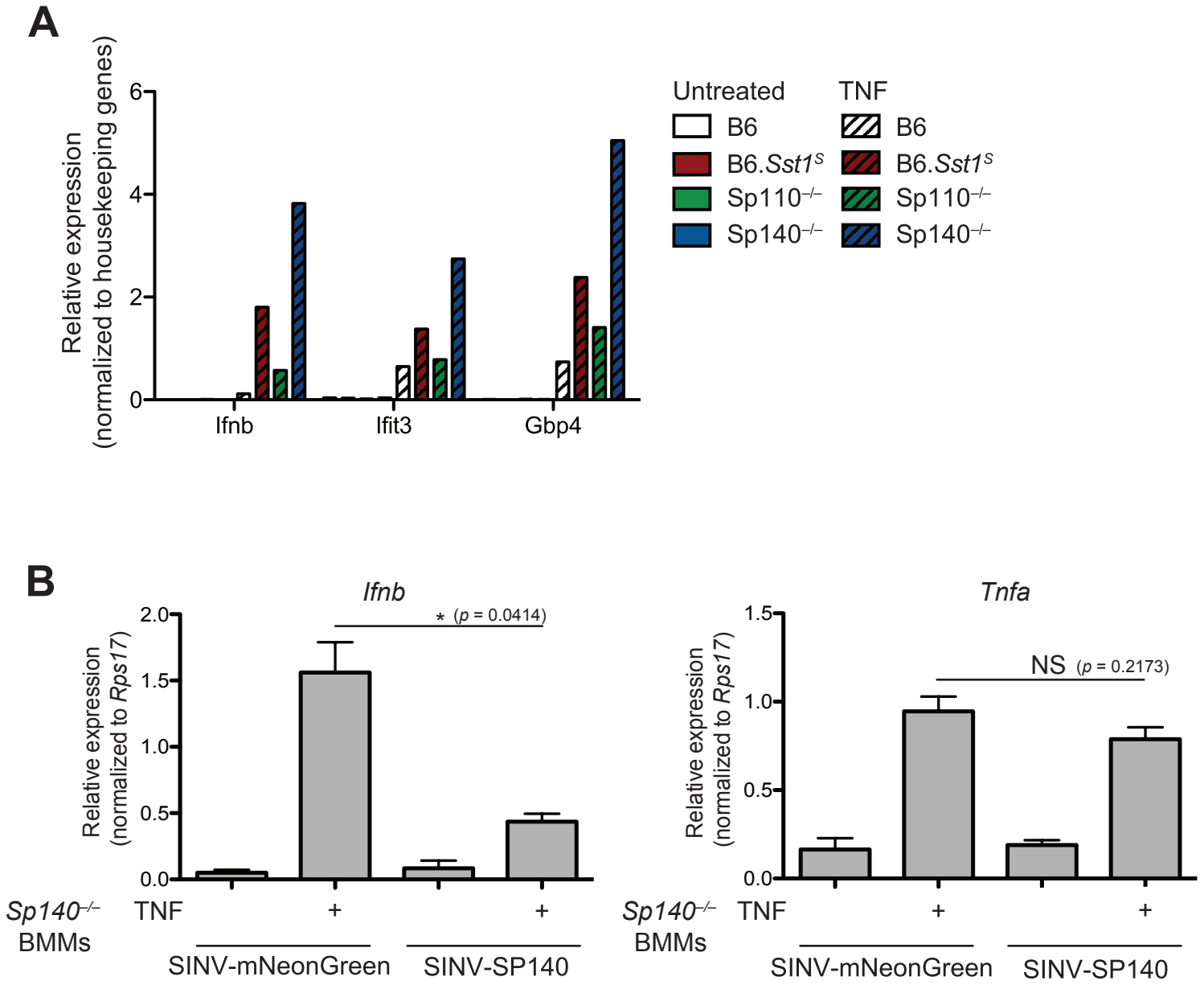

Figure 2– figure supplement 4. Complementation of hyper type I IFN responses in *Sp140*$^{-/-}$ BMMs. (**A**) BMMs were left untreated or treated with TNF-α for 24 hours. Total RNA was used for RT-qPCR. Averages of technical duplicates for one biological replicate are shown. Data is representative of two independent experiments. (**B**) RT-qPCR of *Sp140*$^{-/-}$ BMMs transduced with either control SINV-minCMV-GAL4-mNeonGreen (SINV-mNeonGreen) or SINV-minCMV-Sp140 (SINV-Sp140), primed with 5 ng/mL IFN-γ for 14 hours and treated with 10 ng/mL TNF-α for 4 hours. Three biological replicates were used for SINV-mNeonGreen conditions, and 4 biological replicates were used for SINV-Sp140 conditions. *, $p \leq 0.05$ calculated with an unpaired t-test with Welch's correction. Data are representative of two independent experiments.

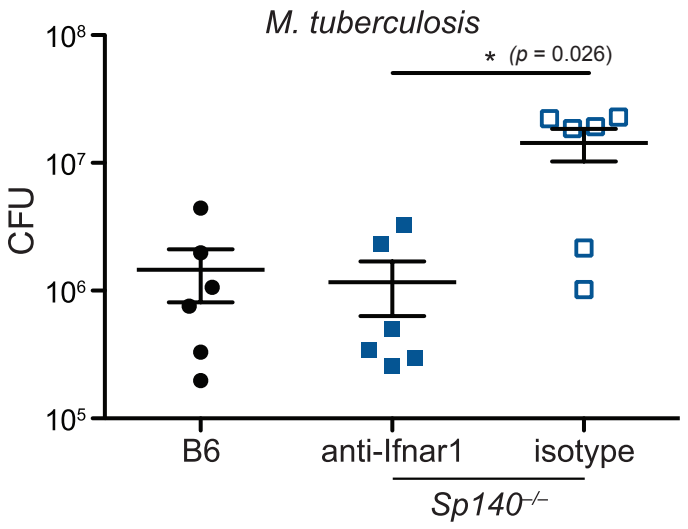

Figure 5 – figure supplement 1. Antibody blockade of IFNAR1 reduces bacterial burden in *Sp140*$^{-/-}$ mice during *M. tuberculosis* infection. Mice were infected with *M. tuberculosis* and treated with either IFNAR1-blocking antibody or isotype control starting 7 days post-infection. At 25 days post-infection lungs were harvested to enumerate CFU. Results of one experiment. All mice were bred in-house. Mann-Whitney test, *, $p \leq 0.05$; **, $p \leq 0.01$; ***, $p \leq 0.005$.